Trans. JWRI, Vol. 24 (1995), No. 1

Review of Mechanical and Metallurgical Investigations of M-A Constituent in Welded Joint in Japan†

Fukuhisa MATSUDA*, Kenji IKEUCHI**, Yasuto FUKADA***, Yukuhiko HORII****, Hitoshi OKADA*****, Toyoaki SHIWAKU******, Chiaki SHIGA*******, and Shinichi SUZUKI********

Abstract

Recent researches reported in Japan on the M-A constituent in the weldment are reviewed. Subjects involved are (1) influence of the M-A constituent on the mechanical properties of weld HAZ and weld metal, (2) influence of the M-A constituent on the localized corrosion and stress corrosion cracking, (3) metallurgical features of the M-A constituent, and (4) factors influencing the formation and decomposition of the M-A constituent.

KEY WORDS: (M-A constituent) (Weld HAZ) (Weld metal) (Mechanical properties) (Toughness) (Corrosion resistance) (Microstructure)

1. Introduction

It is generally recognized that the existence of M-A constituent in the weld HAZ seriously reduces the toughness of the welded joint. Therefore, attention has been paid to the formation of M-A constituent when high strength steel is welded with high heat input or through multi-pass welding. In order to prevent the formation of M-A constituent or to eliminate the M-A constituent, many investigations have been made of the M-A constituent so far in Japan. This report summarizes researches published in Japan from 1981 to 1994 on the effects of the M-A constituent on mechanical and stress-corrosion characteristics, metallurgical features of M-A constituent, and prevention and elimination of M-A constituent in the welded joint.

2. Influence of M-A Constituent on Mechanical Properties of Weldments

2.1 Properties of heat affected zone

2.1.1 C-Mn and HSLA steel of TS590 class and less than TS590 MPa

1) Single thermal cycle

The toughness of the heat affected zone (HAZ) depends on its microstructure, and the microstructure changes from fusion line to base metal continuously. In general, coarse-grained HAZ near the fusion line shows the lowest toughness, and toughness deteriorates over a wide region in the HAZ, when heat input is large as shown in **Fig. 1** [1,2].

A typical SH-CCT diagram of 490 MPa class steel is shown in **Fig. 2** [3]. Microstructure in the HAZ mainly consists of ferrite (grain boundary ferrite, ferrite side plate), bainite(upper bainite, lower bainite) and martensite. It is well known that upper bainite and/or ferrite side plate gives low toughness because of a large fracture facet size and the presence of M-A constituent between lath boundaries. In particular, the existence of

† Received on July 21, 1995
* Professor
** Associate professor
*** Iron & Steel Research Laboratories, Sumitomo Metals Industry, Ltd.
**** Steel Research Laboratories, Nippon Steel Co. (Now at Japan Power Engineering and Inspection Coporation)
***** Manufacturing Department, Kurimoto, Ltd.
****** Steel Plate & Sheet Development Department, Kakogawa Works, Kobe Steel, Ltd.
******* Iron & Steel Research Laboratories, Kawasaki Steel Co.
******** Materials and Processing Research Center, NKK Co.

Transactions of JWRI is published by Welding Research, Institute, Osaka University, Ibaraki, Osaka 567, Japan.

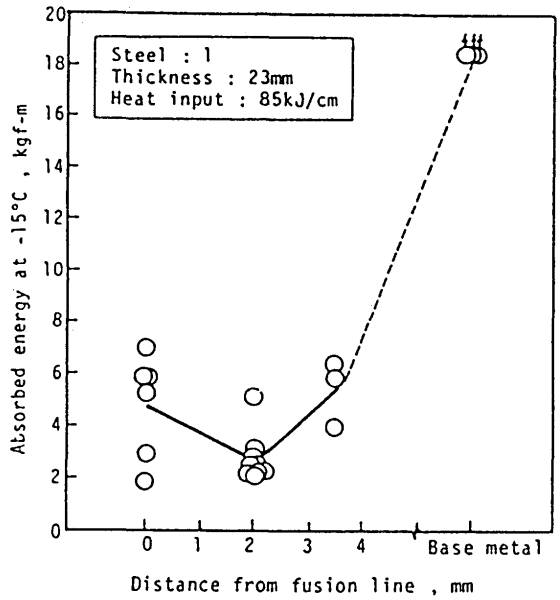

Fig. 1 Impact properties of high heat input weldment of Cu-Ni-Mo-V type steel.

M-A constituents in lath boundaries accounts for the inferior toughness of upper bainite in comparison with lower bainite. The M-A constituent affects the HAZ toughness more than the fracture facet size, as shown in **Fig.3** [2].

Microstructure near the fusion line in 490 MPa class steel mainly consists of upper bainite, and then consists of mixed structures of upper bainite and ferrite(grain boundary ferrite, ferrite side plate). Therefore, an important subject is the improvement of low temperature toughness in the HAZ through control of microstructure.

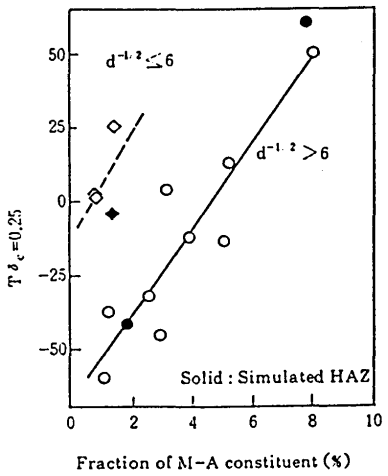

Fig. 3 Relationship between M-A constituent fraction and crack initiation temperature.

2) Multi thermal cycle

In general, a weld HAZ has a complex distribution of microstructure and toughness, because of the multiple thermal cycles resulting from multi-pass welding. API-RP-2Z and EEMUA 150 HAZ CTOD test procedures give a detailed classification of microstructure in the HAZ. The effect of subsequent passes on microstructure near fusion line is schematically shown in **Fig. 4** [4].

Coarse-grained (CG) HAZ microstructure along the fusion line is classified according to the reheating temperature of the subsequent pass. The CG HAZ not reheated by a subsequent pass is called unaltered CG HAZ

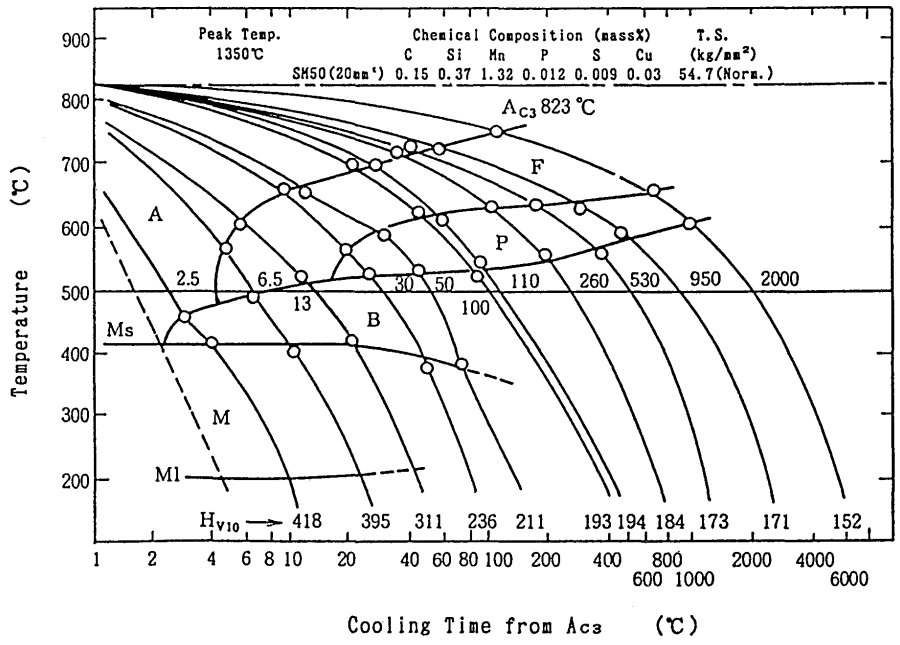

Fig. 2 Typical SH-CCT diagram of TS490MPa class steel.

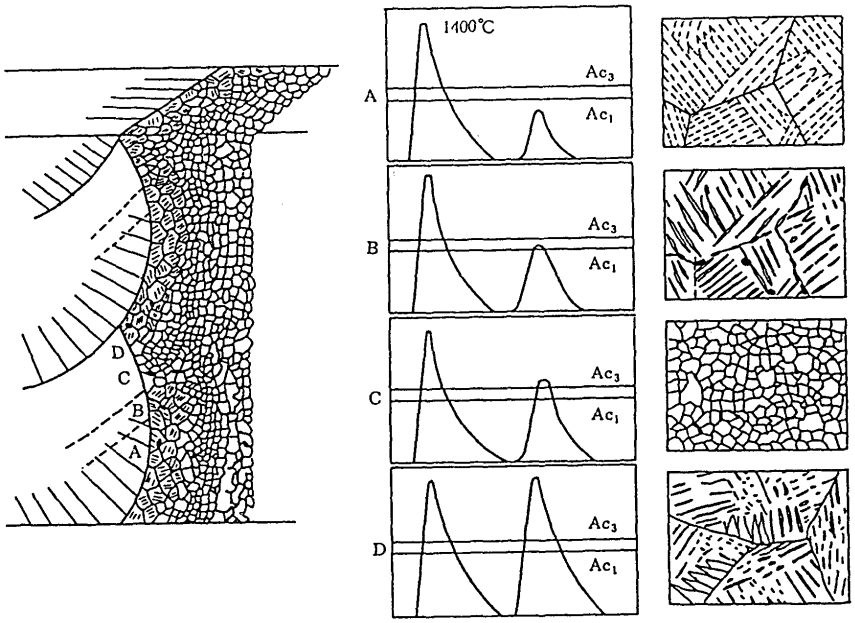

Fig. 4 Schematic diagram showing relation between microstructure and thermal cycle in HAZ.

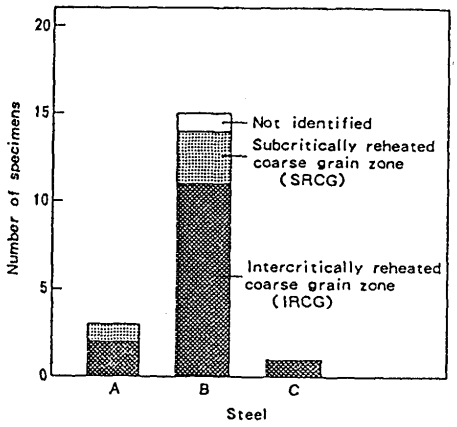

Fig. 5 HAZ microstructure of fracture initiation point in weld HAZ CTOD test specimens (heat input: 4.5kJ/mm).

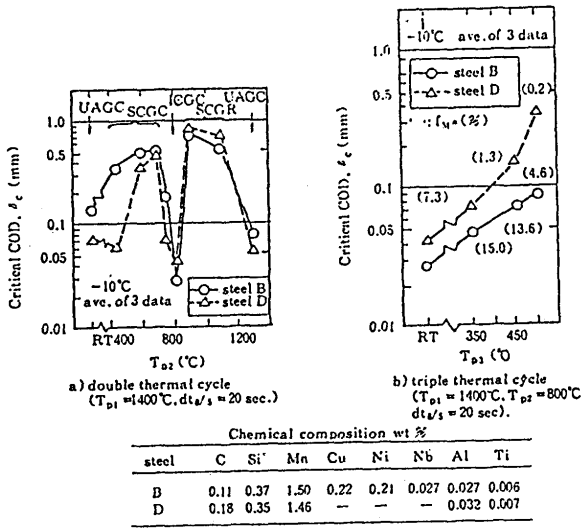

Chemical composition wt %

steel	C	Si	Mn	Cu	Ni	Nb	Al	Ti
B	0.11	0.37	1.50	0.22	0.21	0.027	0.027	0.006
D	0.18	0.35	1.46	—	—	—	0.032	0.007

Fig. 6 CTOD values of simulated HAZ.

(UACG HAZ). However, the CG HAZ reheated to temperatures below A_{c1} is called subcritical-reheated CG HAZ (SRCG HAZ). The region reheated to austenite-ferrite dual phase region (between A_{c1} and A_{c3}) is called intercritically reheated CG HAZ (IRCG HAZ). The SRCG and IRCG HAZ inherit the coarse-grained upper bainitic structure but their second phases are changed. The region reheated to temperatures just above A_{c3} and transformed into fine ferrite-pearlite microstructure is called fine-grain HAZ (FG HAZ). These regions are again reheated below A_{c1} by the subsequent passes.

Figure 5 shows the result of structural analysis at crack initiation points of CTOD specimens [5]. Most of the brittle fractures with low CTOD were initiated from the IRCG HAZ. Considering that the size of the IRCG HAZ is very small, the IRCG HAZ should be recognized as the most brittle zone in the HAZ, containing a very brittle phase. **Figure 6** shows a result of simulated HAZ CTOD test for reproducing the toughness distribution along the fusion line[6]. The first peak temperature is kept constant at 1673 K (1400°C). The HAZ toughness is reduced by a second thermal cycle heating to 1073 K (800°C) (IRCG HAZ) and 1673 K (1400°C) (UACG HAZ). IRCG HAZ is the most important region in the HAZ, because UACG HAZ is formed only by the final pass. The toughness is improved by the third thermal cycle with a peak temperature over 623 K (350°C), because M-A constituents are decomposed into cementites and ferrites.

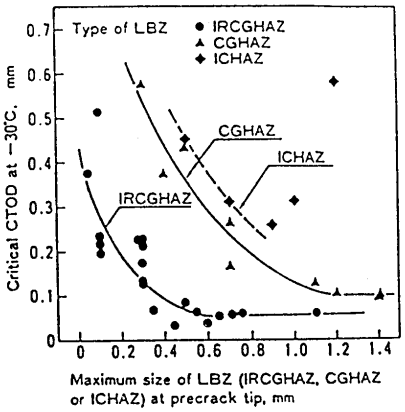

Fig. 7 Effect of maximum size of LBZ at precrack tip on critical CTOD.

Therefore the deterioration of toughness in IRCG HAZ is due to the formation of M-A constituent. Although the multi-pass weld HAZ has a local brittle zone of IRCG, SRCG and UACG HAZs, the IRCG HAZ is the most decisive region in spite of its smallness. **Figure 7** shows effects of the type and size of LBZs on critical CTOD [7]. The IC HAZ represents structure heated to intercritical region resulting from the first thermal cycle. Every LBZ lowers the CTOD value in proportion to its size.

3) Influence of M-A Constituent on Toughness

The metallurgical factors for the improvement of

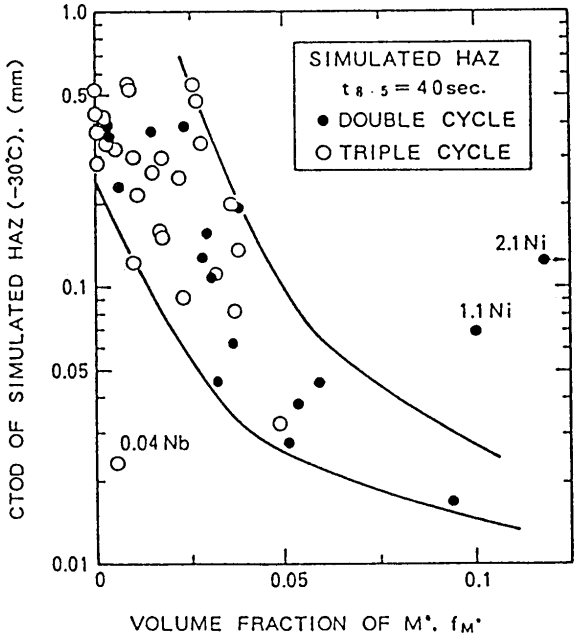

Fig. 8 Dependence of HAZ CTOD on volume fraction of M-A constituent (M*) for simulated IRCGHAZ.

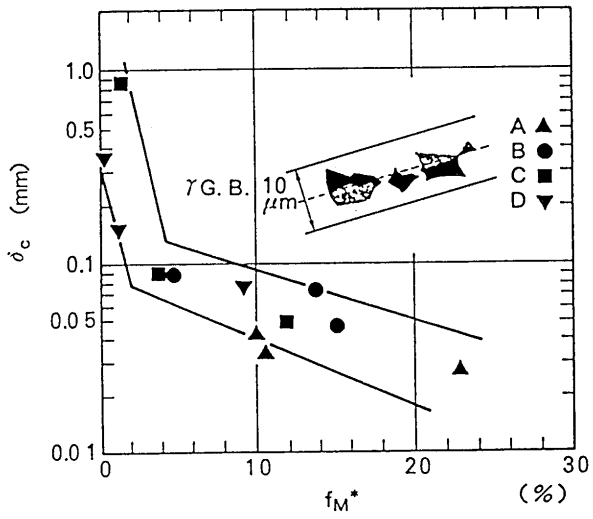

Fig. 9 Relation between critical CTOD and area fraction of M-A constituent for simulated HAZ (triple cycle: T_1=1400, T_2=800, T_3=350, 450, 500°C)

HAZ toughness are classified as follows: (1)refinement of effective grain size (fracture facet size), (2)decrease in M-A constituents and (3)reduction of impurities. The deterioration of HAZ toughness by M-A constituents in the IRCG HAZ occurs in any grade steels, and both Charpy transition temperature and critical CTOD property are reduced with increasing fractions of M-A constituent [2, 4, 5, 8-11, 12-15]. Moreover, a close relation is observed between the CTOD value and the fraction of the decomposed M-A constituent at prior austenite grain boundary as shown in **Figs.8 and 9** [5, 16]. The M-A constituent is formed preferentially at the grain boundary, and stress is more likely to be concentrated at the grain boundary region than at the intragranular region by dislocation pile-up. However, it has been reported that the effect of M-A constituent on

Table 1 Summary of coefficient (B) for transition temperature of FATT & $T_{0.25}$ determined with M-A constituent content (%MA).

FATT	Tδc	ref.
3. 4	10. 3	8)
12. 0	30. 0	10)
−	14. 0	2)
7. 5	−	11)
25. 9	−	12)

$\left.\begin{matrix} vTrs \\ T\delta c \end{matrix}\right\}$ = A + (B) x (%MA)

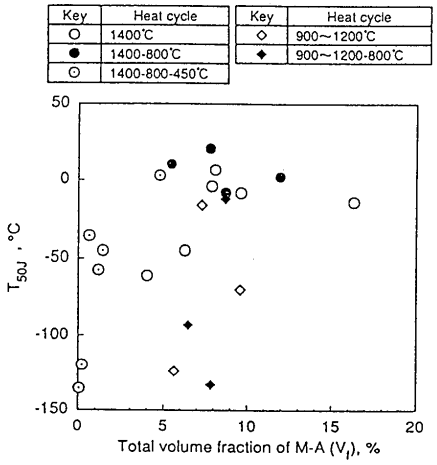

(a) Total fraction of M-A constituent

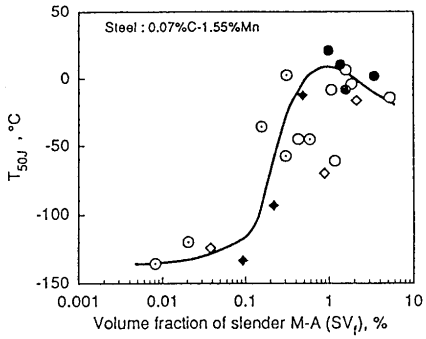

(b) Fraction of slender M-A constituent

Fig. 10 Effect of volume fraction of M-A constituent on LBZ toughness: (a) total fraction of M-A constituent and (b) fraction of slender M-A constituent.

toughness is insignificant in the fine structure such as base metal[17, 18]. Assuming that the Charpy transition temperature (FATT) and CTOD property are linear

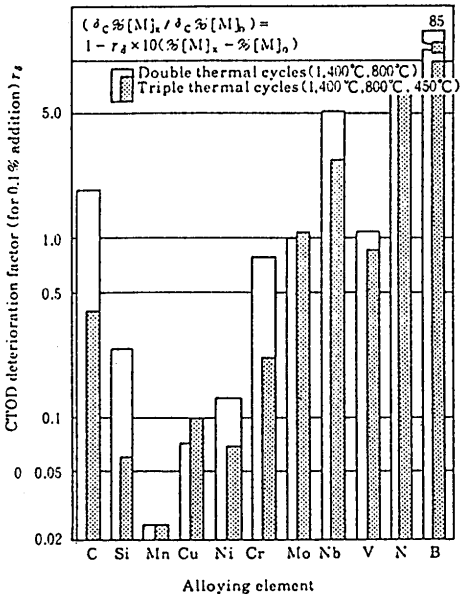

Fig. 11 Comparison of alloying elements in terms of effect on CTOD.

functions of the fraction of M-A constituent, the values of coefficient B (see the equation below the table) obtained are shown in **Table 1**. An example of results is shown in Fig. 3. The coefficient for CTOD property is much larger than that for FATT. This result indicates that the M-A constituent takes part in the initiation of the brittle fracture.

Then, based on fracture behavior, the morphological effect of M-A constituent should be discussed. When M-A constituent with an aspect ratio greater than four was defined as slender (elongated) M-A constituent, the slender M-A constituent influenced the HAZ toughness more seriously than total content of M-A constituent as

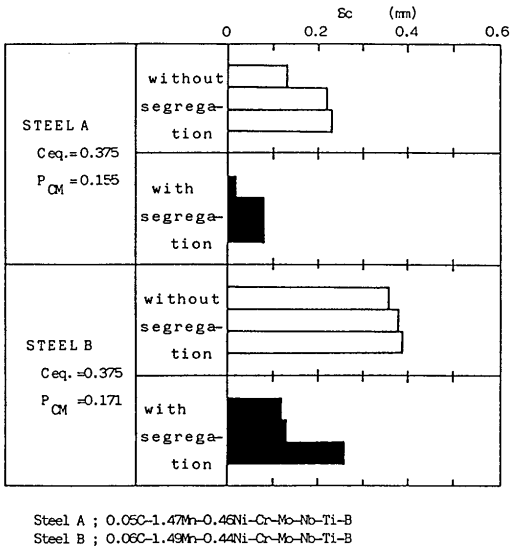

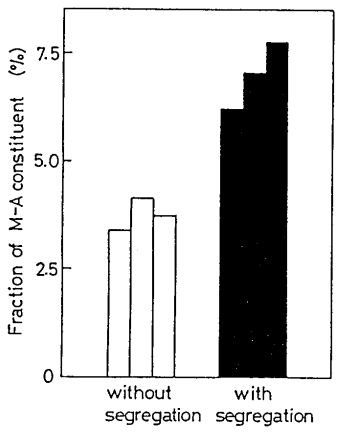

Fig. 12 Effect of segregation on critical CTOD values of simulated HAZ.

Chemical compositions of steels examined.

Steel	C	Si	Mn	P	S	Al	Cu	Ni	Nb	Ceq	Pcm
TM1	0.07	0.11	1.45	0.010	0.001	0.035	0.26	0.73	0.012	0.38	0.17
TM2	0.08	0.38	1.46	0.004	0.001	0.033	0.20	0.20	0.025	0.35	0.18
NM	0.16	0.37	1.49	0.011	0.003	0.017	-	0.16	0.027	0.42	0.26

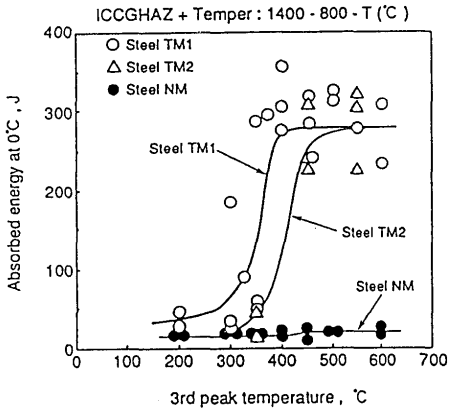

Effect of the 3rd peak temperature on toughness of ICCGHAZ.

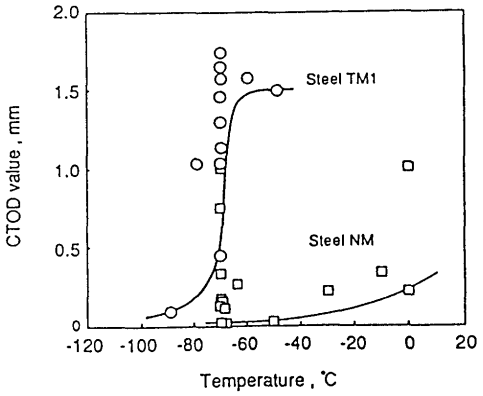

Transition curves of CTOD value for steels TM1 and NM when interpass temperature was 25℃.

Fig. 13 Effect of Si content on toughness of simulated HAZ.

shown in **Fig. 10** [15]. On the other hand, it has been proposed that the maximum size of M-A constituent is not a unique metallurgical factor which reduces the toughness, and mean free path and the statistical distribution of the M-A constituents have also a great influence on cleavage fracture toughness [19].

In order to reduce M-A constituent, it is important to reduce the alloying elements which tend to form M-A constituent. The tendency of various elements to form M-A constituent is shown in **Fig. 11** [4]. M-A constituent is formed more easily by adding B, N, C and carbide forming elements such as Mo, Nb and V, because carbide forming elements retard the diffusion of carbon during transformation from austenite to ferrite and hence the decomposition of M-A constituent. Moreover, it has been reported that the decrease in those elements is important because their segregation leads to the formation of M-A constituents as shown in **Fig. 12** [20]. Segregation is classified into two categories: the first occurrs during solidification for elements such as Mn, Ni, P and S, and the second occurs during transformation from austenite to ferrite, and applies to elements such as C, N and B. The effect of Mn on the formation of M-A constituent is less significant than the effect of other elements [21, 22].

Reduction of Si content suppresses the formation of M-A constituent [23], and promotes the decomposition of M-A constituent with lower peak temperatures of a third thermal cycle [24]. As shown in **Fig. 13** [25], both Charpy impact properties and CTOD properties are improved by decreasing Si content. A similar effect is observed with reducing Al content as shown in **Fig. 14** [26]. It has been reported that the effect of decreasing Al content on the improvement of HAZ toughness is attributed to increased diffusion of carbon, and fine ferrite microstructure without M-A constituent [26, 27].

The increase in chemical compositions enhances the formation of M-A constituent in most cases. Accordingly, it is important to reduce carbon equivalent and solute segregation in steel.

The yield and tensile strength increase with increasing the fraction of M-A constituent [14]. However, it has been reported that the effect of M-A constituent on the strength is less obvious than on the

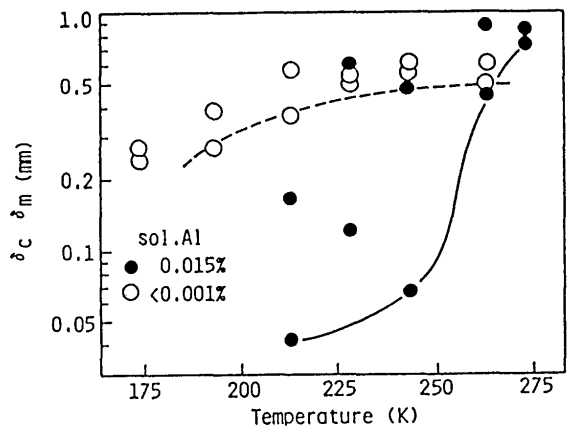

Fig. 14 Effect of Al content on HAZ CTOD values of welded joint.

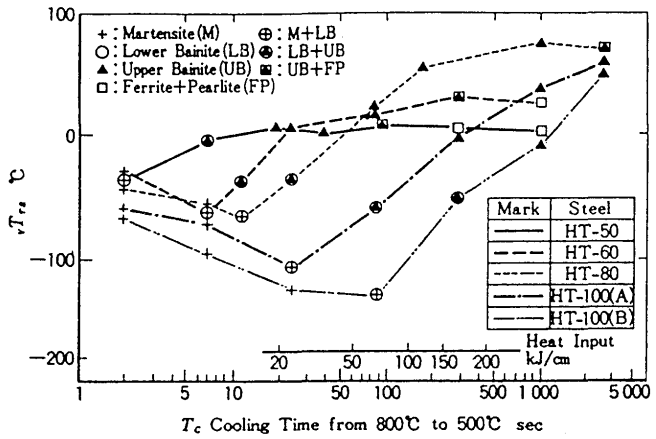

Fig. 15 Effect of cooling time on toughness and microstructure in simulated CGHAZ of various steels.

toughness.

2.1.2 High strength steel of TS590-980MPa classes and special steel

Effects of thermal cycle condition on simulated HAZ toughness in relatively high alloy steels such as TS 590 to 980MPa class high strength steels, steels for pressure vessels, and steels for low temperature service are different from those in TS 490MPa class low alloy steel. HAZ toughness in relatively high alloy steel has been described in relation to M-A constituent and microstructure.

1) Single thermal cycle

Figure 15 shows the effect of cooling time ($\Delta t_{8/5}$) on the toughness of simulated coarse grained HAZ (CGHAZ) (peak temperature = 1623 K (1350°C)) of TS490 to 980MPa class steels (HT-50 to HT-100) [28]. In the case of TS490MPa steel, fracture appearance transition temperature (FATT, vTrs) rises with increase in cooling time. On the other hand, in case of TS590 to TS980MPa class steels, FATT decreases for very short cooling times $\Delta t_{8/5}$, and subsequently increases with cooling time after passing through a minimum value depending on the type of steel. The microstructure of the steels with tensile strengths higher than 590MPa changes greatly with cooling time. The changes in toughness of these steels roughly correspond to their microstructural change irrespective of strength of the steels. The microstructures with martensite and lower bainite (M+LB) lead to the best toughness. With increases in cooling time, the toughness deteriorates drastically according to changes in microstructure from martensite and lower bainite structure to upper bainite (UB) structure. **Figure 16** shows effect of cooling

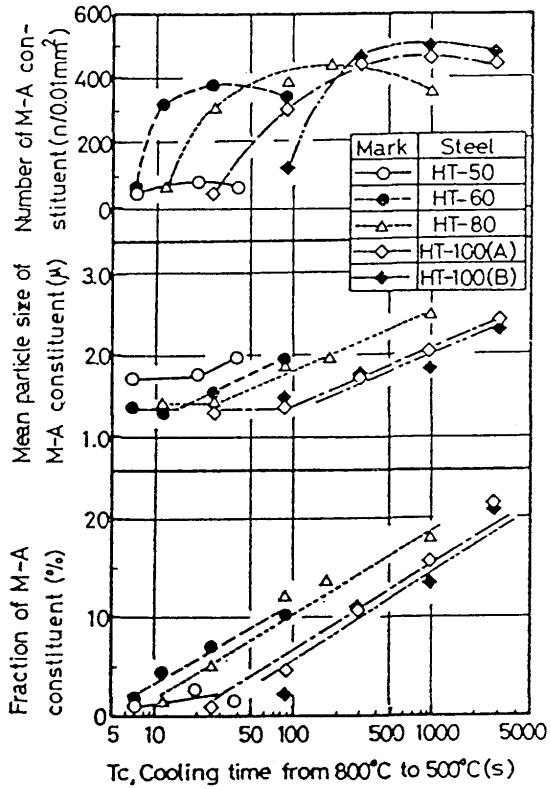

Fig. 16 Effects of cooling time on number, size, and fraction of M-A constituent in simulated CGHAZ of various steels.

time on number, size and fraction of M-A constituent when the microstructure changes from martensite and lower bainite structure to upper bainite structure [28]. In case of TS490MPa (HT-50) steel, cementite and small amounts of M-A constituent form at the inter-lath regions of upper bainite structures. In the case of TS590(HT-60) to TS980MPa(HT-100), large amounts of

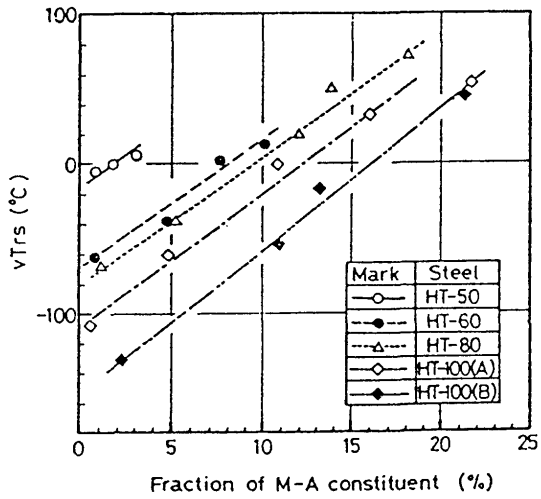

Fig. 17 Relation between toughness and fraction of M-A constituent in simulated CGHAZ of various steels.

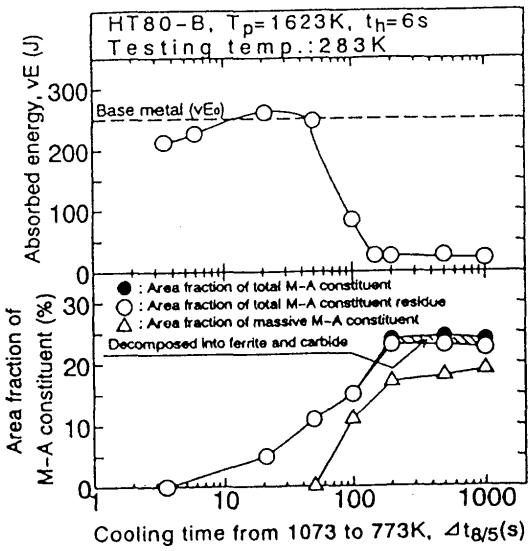

Fig. 18 Relations between vE and $\Delta t_{8/5}$ and between fraction of M-A constituent and $\Delta t_{8/5}$ for HT-80 steel.

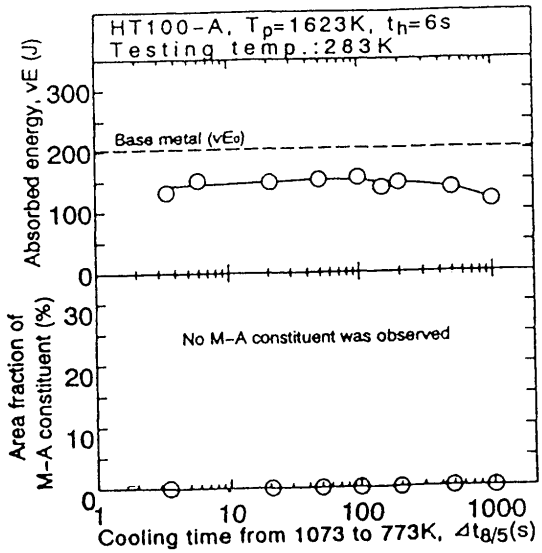

Fig. 19 Relations between vE and $\Delta t_{8/5}$ and between fraction of M-A constituent and $\Delta t_{8/5}$ for HT-100 steel.

M-A constituent form at the inter-lath regions of upper bainite structures. For shorter cooling times, the number of fine M-A constituent particles increases drastically with increase in cooling time. Then, as cooling time increases, the particle size of the M-A constituent increases. Therefore, the fraction of M-A constituent, which is the product of number and size, increases with increase in cooling time. In the various strength steels, there is good correlation between the FATT (vTrs) and the fraction of M-A constituent, while the correlation between the FATT and the number or the size of M-A constituent is rather poor, as shown in **Fig. 17** [28]. This indicates that the HAZ toughness of various strength steels is controlled mainly by the fraction of M-A constituent. However, the toughness level depends on the strength of steels, and shows a tendency to improve with increase in strength. This toughness improvement may be caused by the improved toughness of the matrix with increases in the content of alloying elements such as Ni [28].

Figure 18 shows the effect of cooling time on Charpy absorbed energy (vE) and area fraction of M-A constituent in a TS780MPa steel (HT-80) [29]. The toughness deteriorates for cooling times more than 50 s, according to the formation of M-A constituent as the microstructure changes from martensite and lower bainite structure to upper bainite structure. At the same time, as shown in **Fig. 19**, the toughness of TS980(HT100) does not deteriorate with increase in cooling time, because the upper bainite structure with M-A constituent does not form on account of high hardenability because of high content of alloying elements such as Ni [29].

The M-A constituent is classified morphologically into two types: elongated M-A constituent and massive M-A constituent. For shorter cooling times, only elongated M-A constituent forms in a TS780MPa (HT-80) steel, and vE does not decrease. For slower cooling rate, the fraction of massive M-A constituent increases, and the vE decreases corresponding to the increase in the fraction of massive M-A constituent. This result indicates that the formation of massive M-A constituent is the dominant contributor to the toughness deterioration [29]. However, some reports have shown that the elongated M-A constituent is more detrimental than massive M-A constituent [30-33], and the morphological effect of M-A constituent on toughness has not been fully clarified.

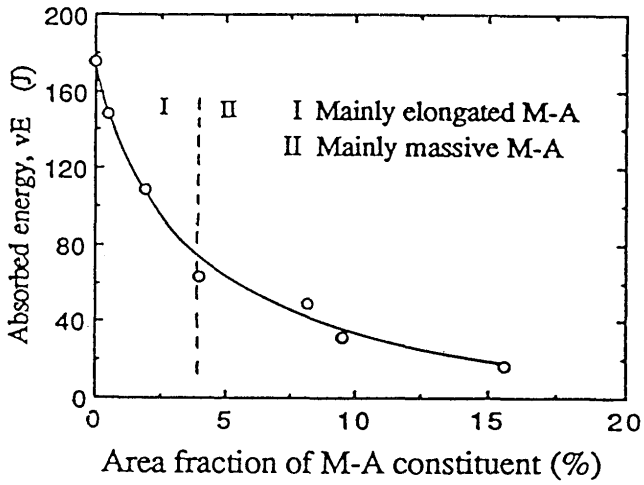

Fig. 20 Relation between vE and fraction of M-A constituent in simulated CGHAZ of 0.19%C-Ni-Mo steel.

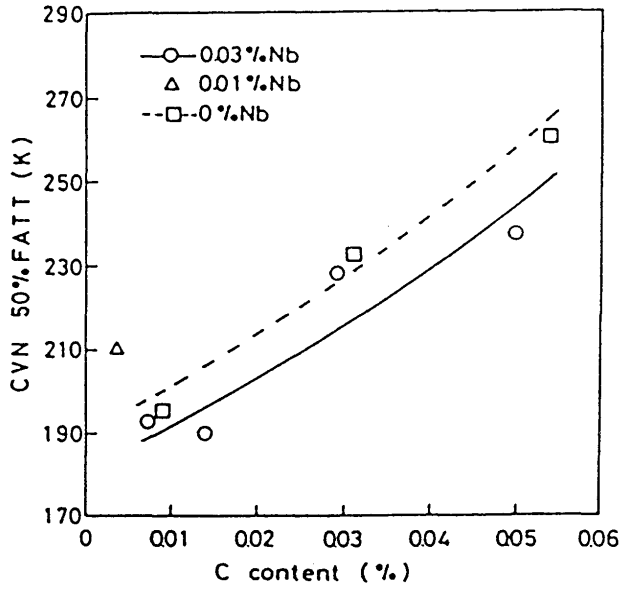

Fig. 21 Effect of C content on FATT in simulated CGHAZ of 2.5%Ni steel.

In the case of Ni-Mo steel (SQV-2A) for pressure vessels with relatively high C content (0.19mass%C), both elongated M-A constituent and massive M-A constituent seriously impair the toughness according to increase in cooling time, as shown in **Fig. 20** [34]. In addition, with increases in cooling time, the width of ferrite laths, prior austenite grain size and fracture facet size also increase [34]. Therefore, vE may be affected not only by the M-A constituent but also by the matrix, because the matrix itself also seems to become brittle with increase in cooling time [34, 35].

Effect of C content on the toughness of the

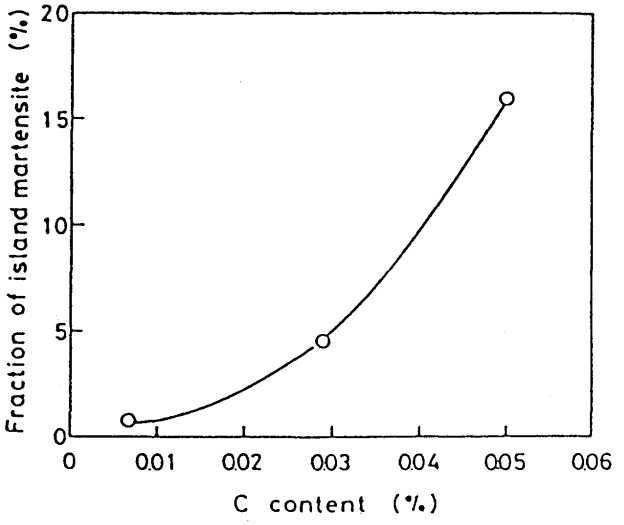

Fig. 22 Effect of C content on fraction of M-A constituent in simulated CGHAZ of 2.5%Ni steel.

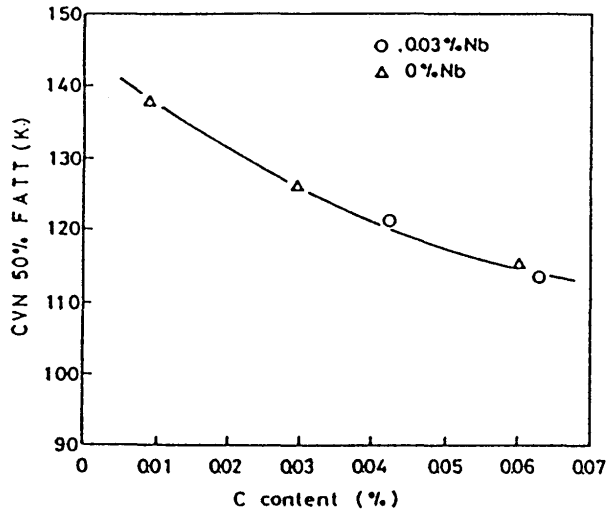

Fig. 23 Effect of C content on FATT in simulated CGHAZ of 9%Ni steel.

simulated HAZ ($\Delta t_{8/5}$: 30s) of 2.5% Ni steel for low temperature service is shown in **Fig. 21** [36]. The toughness improvement with decrease in C content is mainly attributed to decrease in fraction of M-A constituent as shown in **Fig. 22** [36]. On the other hand, in the case of 9%Ni steel, the toughness deteriorates with decrease in C content because of an increase in fracture facet size in spite of a decrease in the fraction of M-A constituent, as shown in **Fig. 23** [36]. This result also indicates that both M-A constituent and the microstructure of matrix are important factors for HAZ toughness.

2) Double thermal cycle

The toughness of CGHAZ resulting from the first thermal cycle changes considerably depending on the peak temperature of the second thermal cycle. **Figure 24** shows the change in toughness of TS 590MPa class high strength steel as a function of the peak temperature of the second thermal cycle[39]. In this figure, the region I represents the ferrite/austenite intercritical region between A_{c1} and A_{c3} (ICCGHAZ), the region II represents the low hardenability region of fine austenite grain (FGHAZ), and region III the high hardenability region of coarse austenite grain (CGHAZ). The deterioration of toughness in the region I is due to the formation of M-A constituent at prior austenite grain boundaries similar to the TS 490MPa class steel. HAZ toughness of high tensile strength steels of more than 590MPa classes is characterized by frequent deterioration of toughness in the fine grained region (region II). In the case of cooling from fine grained austenite, TS490MPa class steel gives high toughness because of transformation into a fine

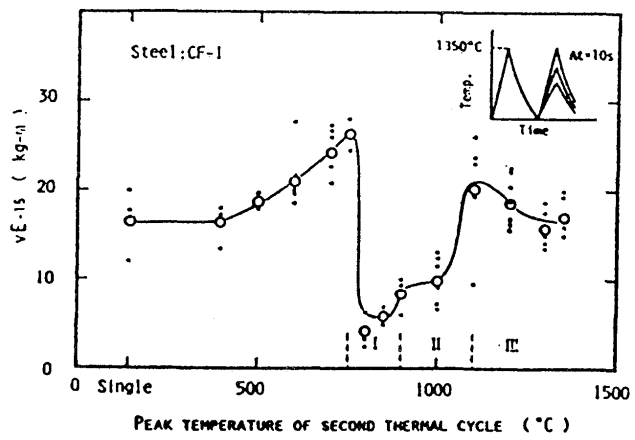

Fig. 24 Relation between toughness and peak temperature of the second thermal cycle in HT-60 steel ($\Delta t_{8/5}$=10 s).

polygonal ferrite structure with less M-A constituent, whereas TS590MPa class steel often gives low toughness because of transformation into a mixed microstructure with ferrite, upper bainite and M-A constituent [37].

The effect of second peak temperature on the toughness of relatively high C-Ni-Mo steel (SQV-2A) is shown in **Fig. 25** [38]. For faster cooling rates ($\Delta t_{8/5}$ = 6 s), the toughness deteriorates in a narrower temperature range, i.e., below 1023 K (750°C) in the intercritical region. For slower cooling rates ($\Delta t_{8/5}$ =

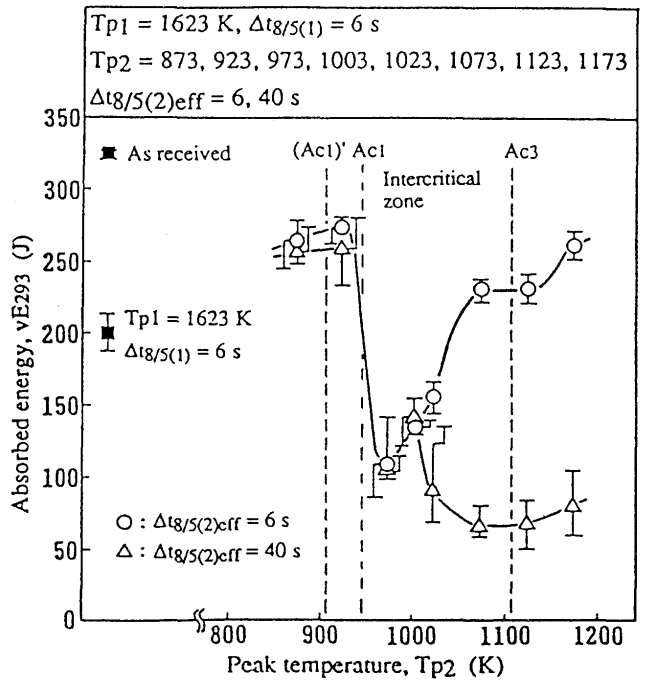

Fig. 25 Effect of peak temperature of second thermal cycle on toughness in 0.19%C-Ni-Mo steel ($\Delta t_{8/5}$=6, 40 s).

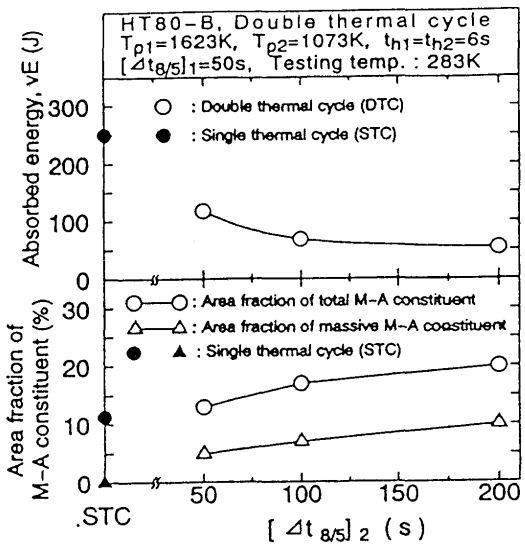

Fig. 26 Relations between vE and $\Delta t_{8/5}$ of the second thermal cycle and between fraction of M-A constituent and $\Delta t_{8/5}$.

40s), the toughness deteriorates over a wider temperature range. This result can be explained as follows: Heating above 1023 K (750°C) leads to reaustenitization of a larger area, and the reaustenitized area transforms mostly into upper bainite structures involving M-A constituent for slower cooling rates, while the reaustenitized area transforms into martensite and lower bainite structures involving less M-A constituent for faster cooling rates [38].

Figure 26 shows the relationships between vE and cooling time and between area fraction of M-A constituent and cooling time, of the second thermal cycle with a peak temperature of 1073 K (800°C) for TS780 steel (HT-80) [29]. This result indicates that toughness deterioration is attributed, not to an increase in elongated M-A constituent, but to an increase in massive M-A constituent. With increases in cooling time, the fraction of M-A constituent increases at the prior austenite grain boundary, which may lead to toughness deterioration [29].

3) Tempering thermal cycle

Figure 27 shows the effect of the peak temperature of the third thermal cycle on vE and area fraction of M-A constituent for a TS780 steel (HT-80) [29]. At reheating temperatures of 673 K (400°C) and 873 K (600°C), the fractions of both elongated M-A constituent and massive M-A constituent decrease, which leads to toughness improvement [29].

PWHT also leads to decrease in M-A constituent and to toughness improvement[39, 40]. **Figure 28** shows a relation between toughness and area fraction of M-A constituent in a TS780 steel (HT-80) [39]. There

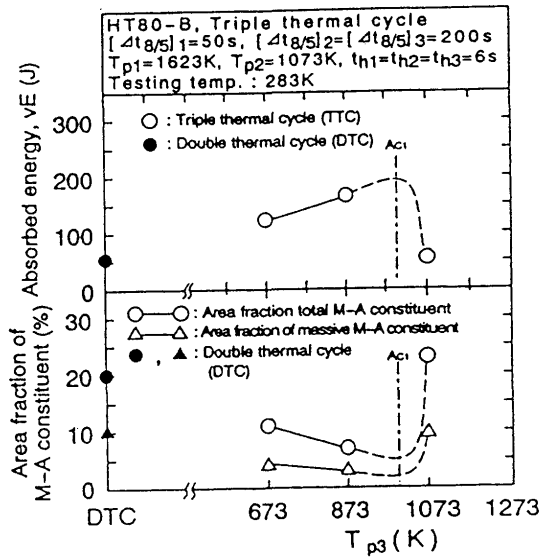

Fig. 27 Relations between vE and peak temperature of the third thermal cycle and between fraction of M-A constituent and the peak temperature for HT-80 steel.

appears to be poor correlation between vE and fraction of elongated M-A constituent, but a good correlation between vE and fraction of massive M-A constituent. Furthermore, the vE of the multi thermal cycle HAZ obeys a relation considerably different from that of single thermal cycle. The value of vE of ICCGHAZ of multi thermal cycle is lower than that of CGHAZ of single thermal cycle. The lower toughness of ICCGHAZ may be attributed to preferential distribution of massive M-A constituent along the prior austenite grain boundaries[39]. **Table 2** shows that the massive M-A constituent decreases the crack initiation and propagation energies much more significantly than the elongated M-A constituent for a TS780 steel (HT-80) [41]. FEM analyses of elastic and plastic strain around a M-A constituent suggest that a region of large tensile plastic strain extended over wider area around the massive M-A constituent than around the elongated [41]. The decrease in Charpy absorbed energy with the increase in cooling time may be attributed to the increase in the interfacial area between massive M-A constituent and the matrix according to the coarsening of the massive M-A constituent [41].

2.2 Properties of weld metal

2.2.1 M-A constituent and toughness

The influence of M-A constituent on mechanical

Table 2 Result of instrumented-Charpy testing on HT-80 steel.

$\Delta t_{8/5}$ s	Total vE J	vE for crack initiation (J)	vE for crack propagation (J)	Area fraction of M-A constituent (%)
50	260	111	130	E:11 . M: 0
200	31	20	7	E: 7 . M:17
(Base metal)	375	105	218	E: 0 . M: 0

E: Elongated M-A constituent
M: Massive M-A constituent

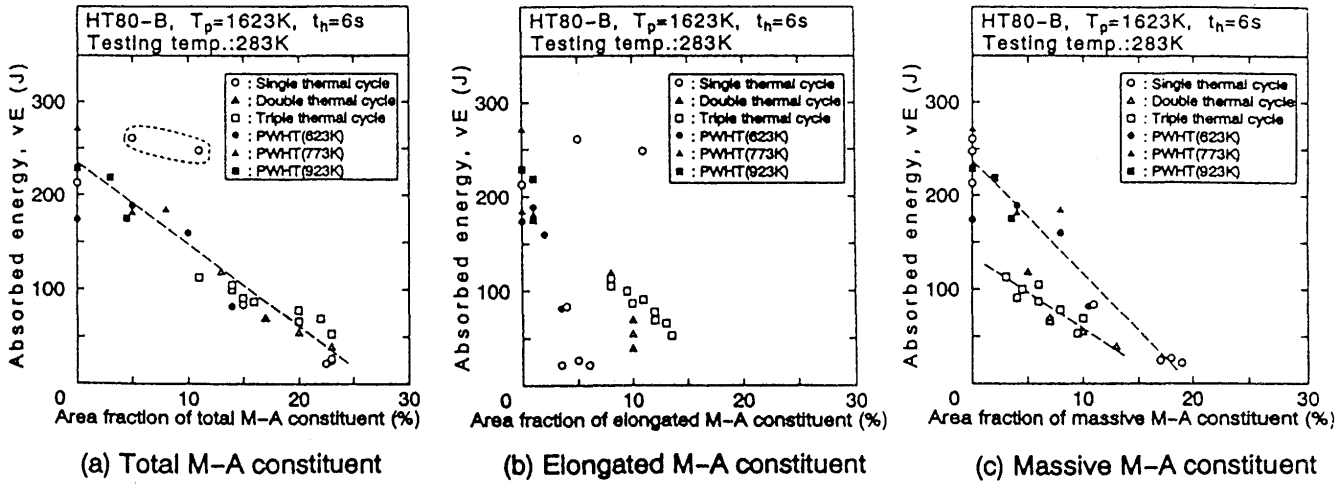

Fig. 28 Relation between vE and fraction of M-A constituent in HT-80: (a) Total M-A constituent, (b) Elongated M-A constituent, and Massive M-A constituent.

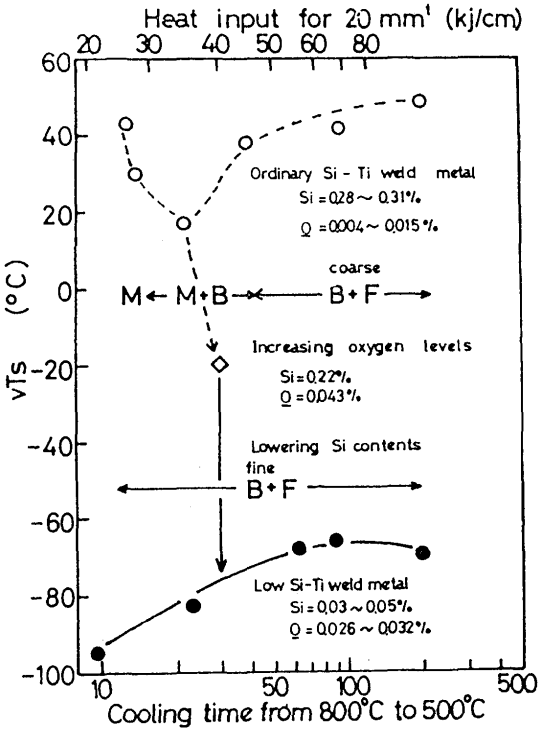

Fig. 29 Relationship between cooling time and FATT of TS780MPa class MIG weld metal.

properties of the weld metals has not been studied as fully as the influence on the heat affected zone. Most of these studies mention that the M-A constituent reduces the weld metal toughness. **Figure 29** shows a relationship between cooling time and FATT of a TS790MPa class MIG weld metal with different silicon and oxygen contents [42]. By reducing silicon content in the weld metal from 0.22mass% to 0.05mass%, the FATT was improved by 60 K in the Charpy impact test. This was explained in terms of a decreased amount of M-A constituent and refined bainitic ferrite size with decreasing silicon content. It was reported that an increase in nitrogen reduces the CTOD properties of both Si-Mn type weld metal and Ti-B type weld metal, as shown in **Figs. 30** and **31** [43, 44]. However, the cause of the toughness deterioration was different between weld metal types. Increase in grain boundary ferrite with increasing nitrogen was said to be the cause of low toughness in the Ti-B bearing system [44]. While microstructural change was not observed by optical microscopy, M-A constituent appeared instead of pearlite with increasing nitrogen in the Si-Mn type weld metal [43]. In the case of Figs. 29 and 30, weld metals were prepared with single run, and it can be said that the increase in M-A constituent is responsible for the toughness deterioration of as-welded columnar structure regions.

Usually, welding is performed with multiple runs,

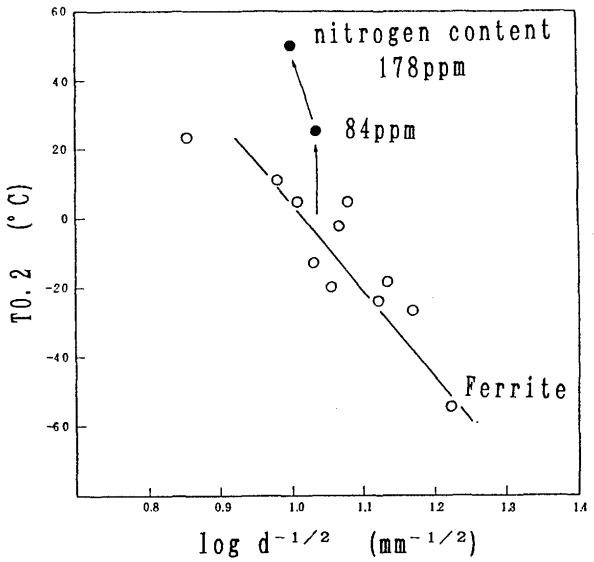

Fig. 30 Relationship between unit crack path and $T_{0.2}$ in Si-Mn-N weld metal.

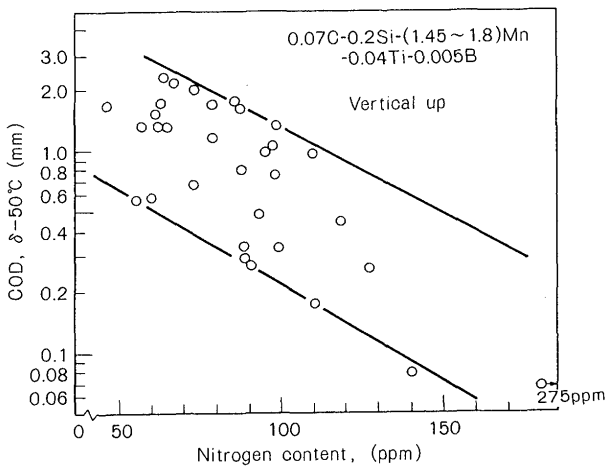

Fig. 31 Influence of nitrogen content on CTOD values at -50°C in Ti-B bearing SMA weld metal.

and weld metals have both as-welded columnar structure zones and reheated zones. Therefore the toughness of reheated weld metal has been studied using a weld thermal cycle simulator. **Figures 32, 33** and **34** show the test results for TS780MPa class low alloy weld metal [45, 46]. M-A constituent increased with increasing carbon content in the weld metal and was formed mostly at 1223 K (950°C) among 1023, 1223, 1623 K (750, 950, 1350°C), and in the as-welded condition (Fig. 32). Absorbed energy reduced gradually with increase in the area fraction of M-A constituent as shown in Fig. 33. Figure 34 shows the effect of a double weld heat cycle on the weld metal toughness of Mn-Mo-Ti-B type for TS490MPa class steel [46, 47]. In Fig. 34, FATT for each peak temperature in the 1st cycle was lowered by

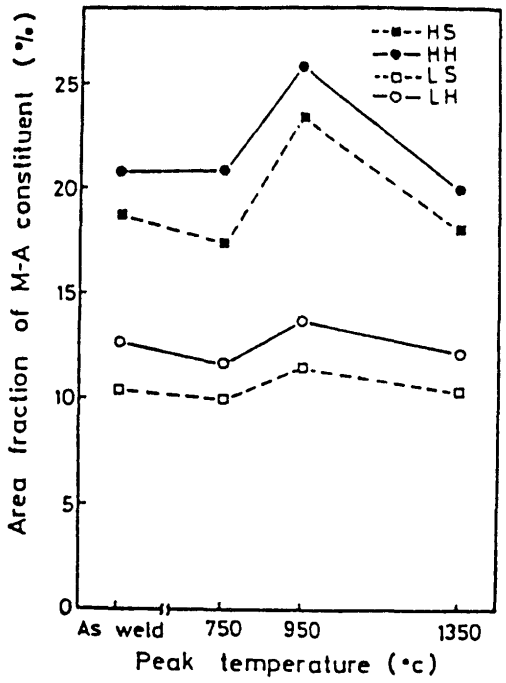

Fig. 32 Effect of peak temperature on M-A constituent of TS780 class weld metal. C contents in weld metals HS and HH are 0.14mass%, and LS and LH 0.06mass%.

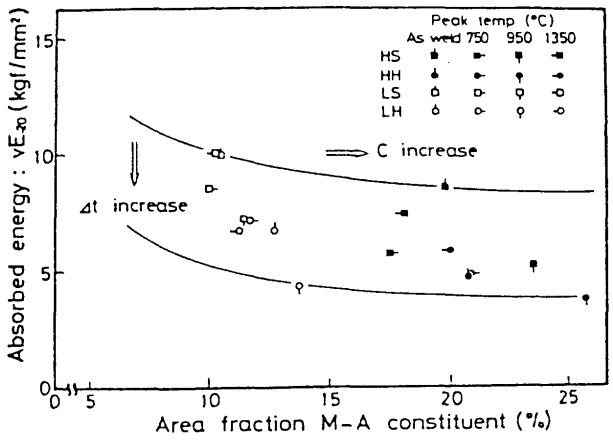

Fig. 33 Relationship between absorbed energy at -20°C and area fraction of M-A constituent.

applying the 2nd cycle with a peak temperature of 823 K (550°C). It was observed that most of M-A constituent was decomposed to pearlite and cementite by applying the 2nd cycle with a peak temperature of 823 K as shown in **Fig. 35**. Therefore, the improvement of toughness in Fig. 34 is due to the decomposition of M-A constituent and the deterioration of toughness by M-A constituent is about 10 to 30 K in FATT. M-A constituent was decomposed by heating up to 823 K (550°C). In the case of multipass welding, M-A constituent decomposes in most of the reheated region as

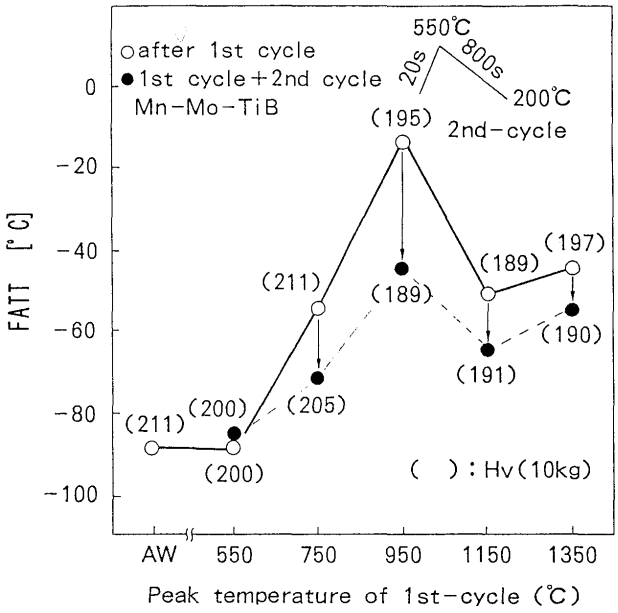

Fig. 34 Effect of 2nd thermal cycle on toughness of Ti-B bearing SA weld metal for TS490MPa class steel.

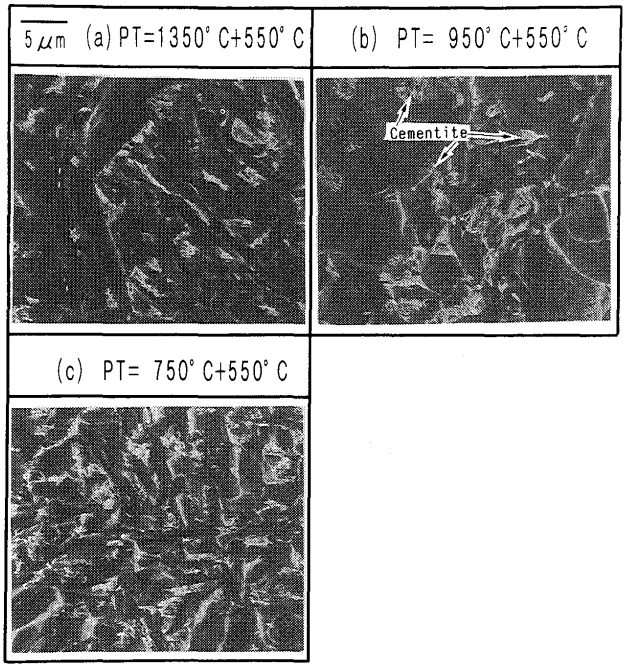

Fig. 35 Second phase of Ti-B bearing SA weld metal after 2nd weld thermal cycle.

a result of the heating of successive welding passes except for the area reheated by the final pass. **Figure 36** shows a relation between M-A constituent area fraction after the 1st cycle and toughness improvement by the 2nd cycle in Fig. 35. Toughness improvement by the 2nd cycle is increased with increasing the amount of M-A constituent after the 1st cycle, obeying the

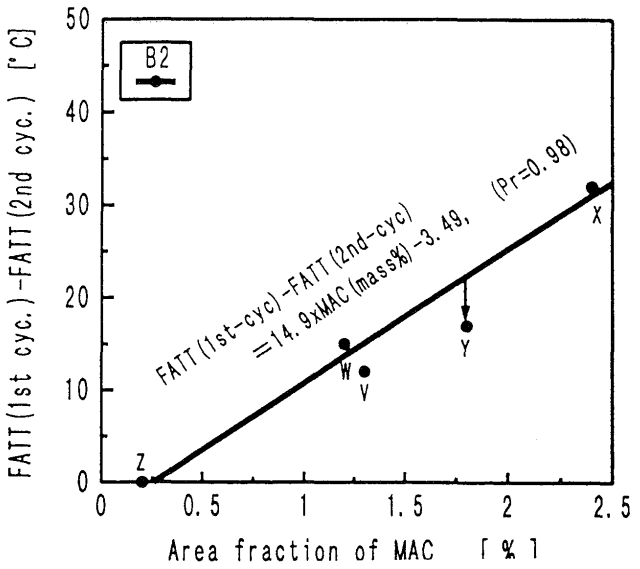

Fig. 36 Relation between toughness increase by 2nd thermal cycle and area fraction of M-A constituent after 1st thermal cycle.

following equation.

$$\Delta FATT = FATT(1st\ cycle) - FATT(2nd\ cycle)$$
$$= 14.9 \cdot MAC(\%) - 3.49$$

2.2.2 M-A constituent and other properties

Most of the reported papers described the effect of M-A constituent on toughness, but they did not refer to properties of weld metals. This is probably due to the difficulty in evaluating the properties because the reheated area is narrow and peak temperature is changed gradually in actual weld joints. The numerals in Fig. 34 represent the Vickers hardness numbers after the 1st and 2nd weld heat cycles. The hardness after reheating to 823 K (550°C) was hardly changed from that before the 2nd cycle, while it decreased after the 2nd cycle at higher reheating temperatures. Considering that the M-A constituent was decomposed to cementite and pearlite at 823 K (550°C) in the 2nd cycle, a hardness decrease after the 2nd cycle is due to M-A constituent. The hardness decrease was less than 9 Hv, and the influence of M-A constituent on the tensile strength can be evaluated to be less than 30MPa.

3. Effect of M-A constituents on the corrosion resistance properties

3.1 Localized corrosion

Effect of M-A constituents on localized corrosion in the HAZ has been investigated by Miyata and Shiga[49, 50]. They made clear that M-A constituents promote localized corrosion because the increase in the amount of the M-A constituent reduces the rest potential. **Figure 37** shows the cross sectional profiles of test pieces after galvanostatic anodic dissolution tests. Test pieces of simulated HAZ involving regions heated to various peak temperatures were prepared with Gleeble heating method for two kinds of steels, steel A and steel B, and were subjected to synthetic corrosion tests by the galvanostatic anodic dissolution testing method. Steels A and B with tensile strength of 550MPa were produced for ships in Arctic regions by TMCP. Corrosion of steel A is remarkable in the temperature range of 1273 K to 1623 K (1000 to 1350°C) in comparison with steel B. M-A constituents are also observed in the HAZ region corresponding to extensive corrosion, and the corrosion depth is proportional to their amount as shown in **Fig. 38**. The result of rest potential measurement shown in **Fig. 39** demonstrates that the rest potential is reduced by increasing amounts of M-A constituent, and the rest potential of steel A is recovered when the HAZ is tempered at 873 K (600°C) to decompose M-A constituents. The ships used in Arctic regions have the problem of localized corrosion in HAZ in the side body because of detaching of paint by abrasion with floating.

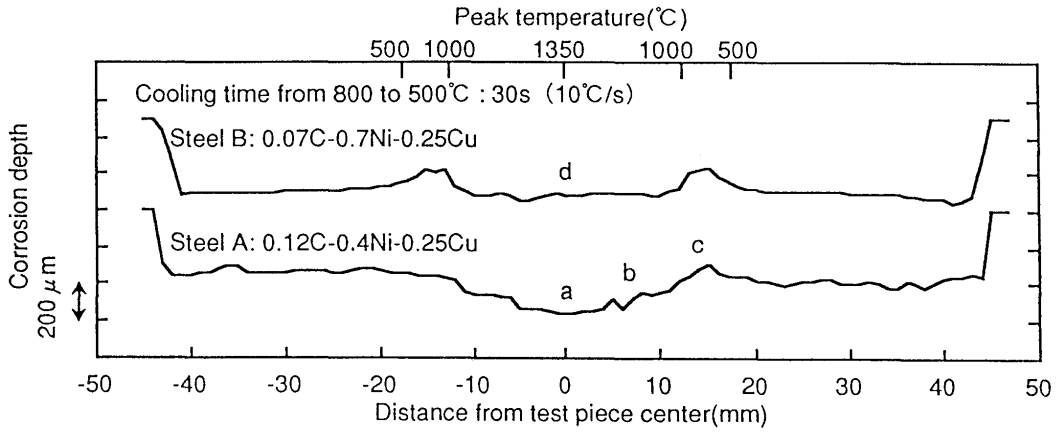

Fig. 37 Cross sectional of test pieces after galvanostatic anodic dissolution test.

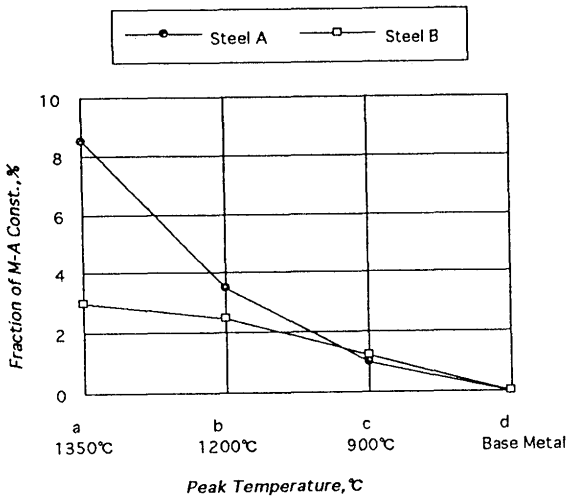

Fig. 38 Relation between fraction of M-A constituents and peak temperature of HAZ.

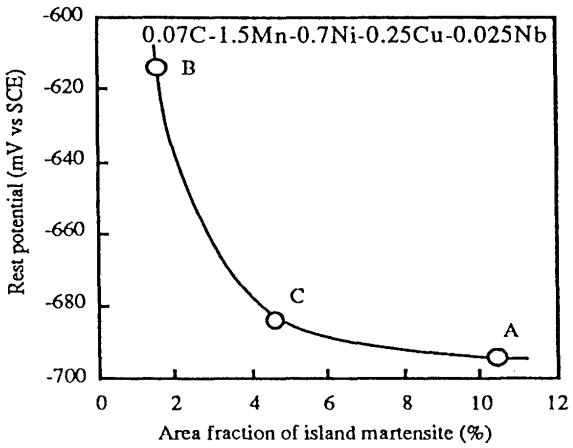

Fig. 39 Relation between rest potential and M-A constituents.

ice. The preferable combination of added Ni content with reduction of M-A constituents, eg., decrease in carbon content, has made it possible to develop the new grades of steel with high resistance to local corrosion in the weldment.

3.2 Stress corrosion cracking

Effect of M-A constituents on stress corrosion cracking has been investigated for the weld HAZ and base hot coil by Kikuta[51, 52] and Yamane[53], respectively. Both researchers insist that M-A constituents create strong traps for hydrogen so that they may lower the critical stress for hydrogen cracking. **Figure 40** illustrates the relationship between the fraction of M-A constituents and critical stress Kth for simulated HAZ of steels with tensile strength of 600MPa. The fraction of M-A constituents was controlled by varying the cooling time, Δt, from 1073 K to 773 K (800 to 500°C) in

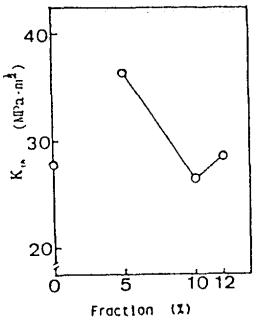

Fig. 40 Relation between Kth and the fraction of M-A constituents.

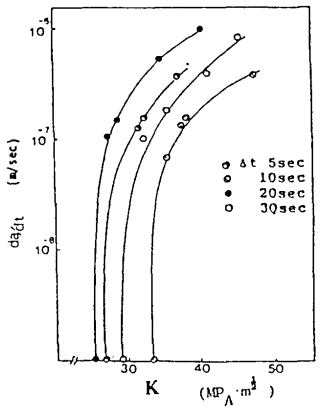

Fig. 41 Relation between crack propagation and K.

simulated thermal cycles with the peak temperature of 1473 K (1200°C). The critical stress of each HAZ was obtained with three point bending tests with a fatigue pre-crack under continuous loading. An increase in the fraction of M-A constituents in a bainitic structure lowers the Kth while the amount below 5% has no harmful effect. The analysis of crack propagation shown in **Fig. 41** demonstrates the high propagation rate in the presence of M-A constituents. In this figure, the fraction of M-A constituents corresponding to cooling times Δt of 30, 20, 10 and 5 s are 11, 10, 5 and 0%, respectively. The observation of crack propagation in the boundary between M-A constituents and bainite supports the hypothesis that the increase in the amount of M-A constituents raises the crack propagation tendency.

Sensitivity to stress corrosion cracking seems to depend on the loading method. Yamane reported that M-A constituents in fractions, even below 2 to 5% will reduce the critical stress of hydrogen cracking in a Shell bend test, NACE TMO 177-90 method B, as shown in **Fig. 42**, but not in a DCB test. He interpreted this phenomenon by considering that the induced stress at the fatigue tip of shell bends is higher than that of DCB

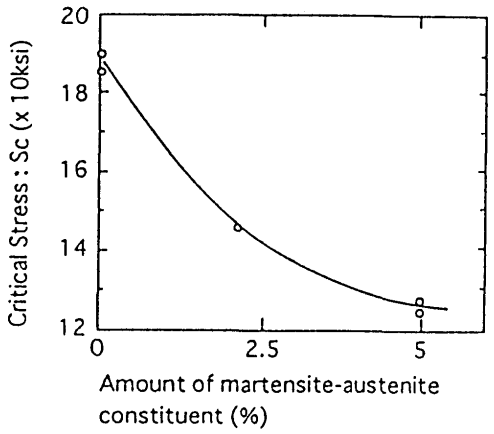

Fig. 42 Relation between critical stress Sc and M-A constituents for line pipe steel.

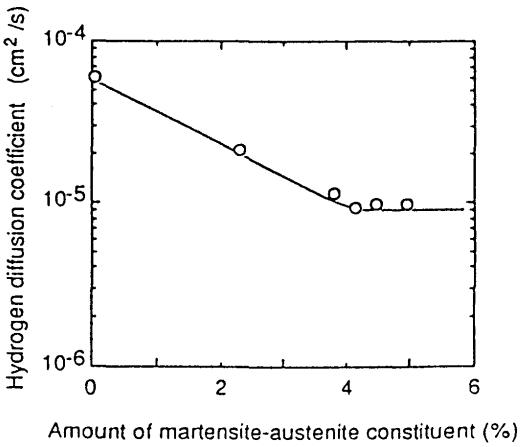

Fig. 43 Relation between hydrogen diffusion coefficient and amount of M-A constituents for line pipe steel.

because constraint force in the former is larger than that in the latter. Both researchers pointed out , as can be seen in **Fig. 43**, that the increase in M-A constituents reduces hydrogen diffusion coefficients because M-A constituents with high dislocation density may become trap sites for hydrogen. In addition they emphasized that the adverse effect of M-A constituents is more serious than that of conventional lath martensite and it disappears when they are tempered at 523 K (250°C) for 3.6 ks (1 hr).

4. Metallurgical features of M-A constituent

4.1 Effect of cooling rate on shape of M-A constituent

Okada et al.[29, 54] investigated the effect of cooling rate on the shape of M-A constituent. The M-A constituent is classified morphologically into two types: massive M-A constituent and elongated M-A constituent as shown in **Fig. 44** [29]. The type of M-A constituent changes with an increase in cooling time, $\Delta t_{8/5}$ (cooling time from 1073 to 773 K) as follows: elongated M-A constituent, elongated M-A constituent + massive M-A constituent, elongated M-A constituent + massive M-A constituent + carbide (see **Fig. 45**) [54].

Since the M-A constituent is formed from the austenite in the final stage of transformation during the cooling process, it may be thought that the formation of the M-A constituent is closely related to the growth of ferrite (α) phase during the cooling process, namely the hardenability of steel. According to observations with an optical microscope, no boundary α phase was formed even for $\Delta t_{8/5}$ of 500s in steels of higher hardenability, and the M-A constituent was formed between lath-shaped α phases.

However, in the steels of lower hardenability, the boundary α phase was formed, but the lath-shaped α phase could not be clearly observed even for $\Delta t_{8/5}$ of 200s or more. In this steel, a lot of coarse massive M-A constituent were formed. Since the boundary α phase and the intergranular elongated α phase grew easily in the steels of lower hardenability, it is conceivable that intergranular elongated α phases grow to contact with each other, leaving untransformed γ phase regions of a massive shape among them. The massive M-A constituent was probably formed from the untransformed γ region of a massive shape during the cooling process. This may explain why the M-A constituent formed in steels of lower hardenability was larger than in the steels of higher hardenability. It can therefore be concluded that the difference in the hardenability causes the difference in the shape of the M-A constituent [54].

4.2 Chemical analysis and hardness of M-A constituent

Higher carbon content and higher hardness of M-A constituent were found by many authors. Biss and Cryderman [55] measured the degree of partition of individual elements, Si, Mo, Mn, and particularly carbon, between the bainitic ferrite matrix and the M-A constituent of hot-rolled law-carbon steels by microprobe analysis. From the results, the high-carbon peaks often exceeded 0.5%C, occasionally exceeded 1%C. However, it appeared that the M-A constituent was the same average composition with respect to all alloying elements other than C.

Komizo and Fukada[8] measured the distribution of carbon content in the HAZ of C-Mn alloyed 490 MPa class steels by EPMA and also measured the Vickers hardness of M-A constituent. The peak points in carbon distribution profiles, corresponding to the M-A

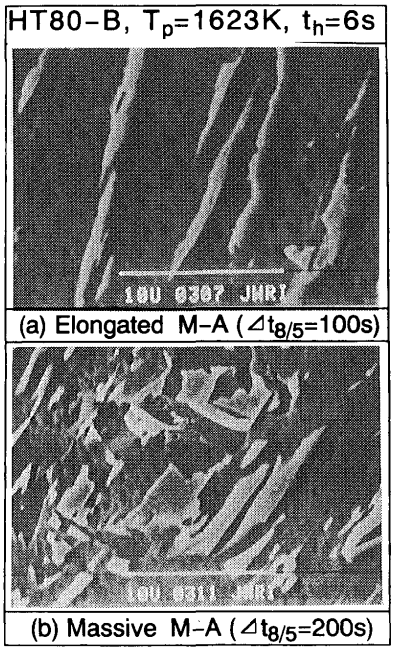

Fig. 44 Examples of morphology of elongated M-A constituent and massive M-A constituent [29].

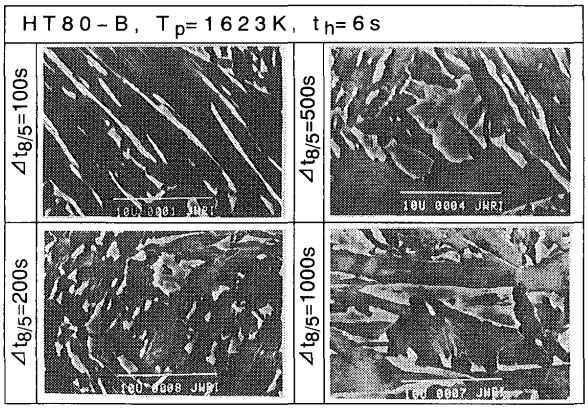

Fig. 45 Comparison of the dimensions and shapes of M-A constituent for different $\Delta t_{8/5}$ [29].

constituent, were 1.07-1.32 mass%, although the carbon contents in the bulk of the base metal were 0.025 - 0.19 mass% (see **Fig. 46**). The hardness of M-A constituent showed higher values of Hv=650-700 than the matrix (see **Table 3**).

Josefsson and Andren [56] found 1.14%C in M-A constituent comparing with 0.005%C in the surrounding ferrite. Moreover they made a calculation of equilibrium content of carbon in retained austenite. They concluded that at 693K where the bainitic reaction ceases, the

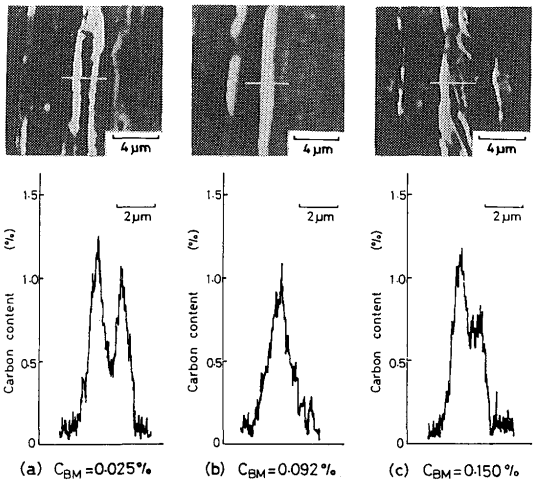

Fig. 46 Results of carbon line analysis by EPMA [8].

Table 3 Hardness in M-A constituent.(Hv=2g) [8].

C content in base metal(%)	Max. Hardness in M-A constituent	Ave. Hardness in base metal
0.025	649	214
0.092	701	221
0.150	693	215

Table 4 Measured carbon content of M-A particle and estimated 0.2% offset yield strength (YS) [57].

Peak temp.(°C) 1st T1	Peak temp.(°C) 2nd T2	Steel	Carbon content (mass%)	Estimated YS (MPa)
1400	–	B	0.34	1565
1400	800		0.44	1735
1400	–	E	0.48	1797
1400	800		0.70	2090

expected carbon concentration in austenite was about 2.6 mass%. In their investigation the bainite start temperature (Bs) was estimated to be 851 ± 5 K, but the transformation started at a low temperature during continuous cooling, between 843 and 693 K.

Kawabata et al.[57] measured the high carbon contents of 0.34-0.70 mass% in CGHAZ or ICCGHAZ of 360-460 MPa class steels by the line analyses(**Table 4**).

Okada et al.[58] investigated the carbon distribution and also the Vickers hardness of the M-A constituent in simulated CGHAZ of 780-980 MPa class HSLA steels. The carbon distribution in M-A constituent analyzed by EPMA area analysis is shown in **Fig. 47**. Carbon is clearly concentrated in the M-A constituent. The changes in the chemical compositions of M-A constituent with $\Delta t_{8/5}$ in simulated CGHAZ of 780-980

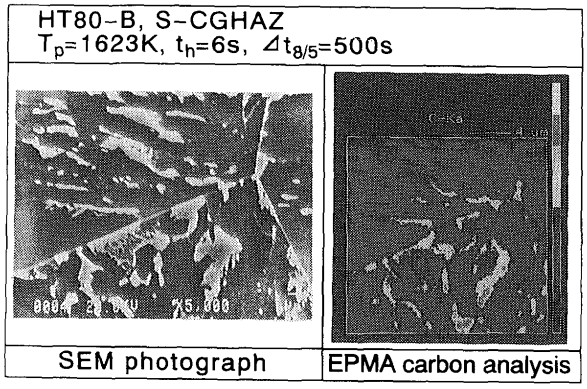

Fig. 47 Distribution of C in M-A constituent of 780 MPa class steel subjected to thermal cycle of $\Delta t_{8/5}$=500s by EPMA [58].

MPa class HSLA steels analyzed by EPMA were shown in **Fig. 48**. The carbon content was much higher than those of the matrix ferrite and the base metal, and increased with $\Delta t_{8/5}$. The Ni content of the M-A constituent was also higher, and increased with $\Delta t_{8/5}$. Thus the M-A constituent tends to be enriched in austenite stabilizing elements C and Ni.

It has been well known that the hardness of the martensite is controlled mainly by its C content. The relation between the Vickers hardness and carbon content of the M-A constituent is shown in **Fig. 49** [58]. The hardness of the M-A constituent was increased with C content. The hardness of the massive M-A constituent (Hv-950) was generally higher than that of the elongated M-A constituent (Hv-700). The hardness and C content of M-A constituent can be reduced significantly by a post weld heat treatment at temperatures from 623 to 773 K.

Thus, the hardness of M-A constituents is very high compared with the matrix. If tensile stress is applied to a steel containing M-A constituents, an

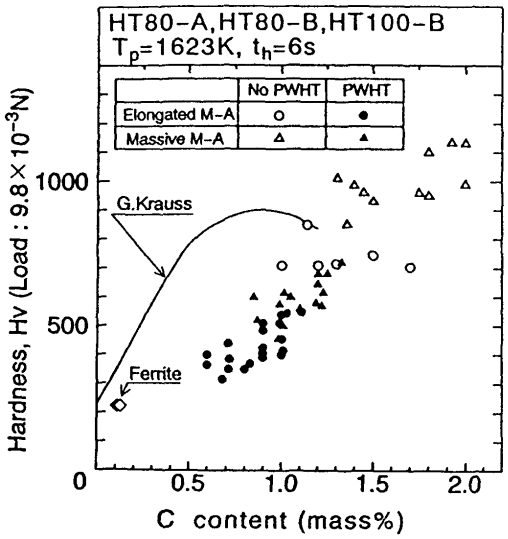

Fig. 49 Relation between Vickers hardness and C content of M-A constituent [58].

excessive internal stress will be generated in the matrix near the M-A constituent because of the concentration of plastic strains resulting from the mismatching of their hardnesses (as long as the M-A constituent itself is not cracked). The concentration of plastic strains near the M-A constituent may play an important role in the initiation and propagation behavior of cleavage fracture.

4.3 Fine microstructure of M-A constituent

It is generally accepted that the M-A constituent consists of martensite (lath and plate martensites) and retained austenite, and may contain cementite precipitated either from austenite or as a consequence of lath martensite self-tempering[59]. However, only little work has been done on a comprehensive analysis of its fine

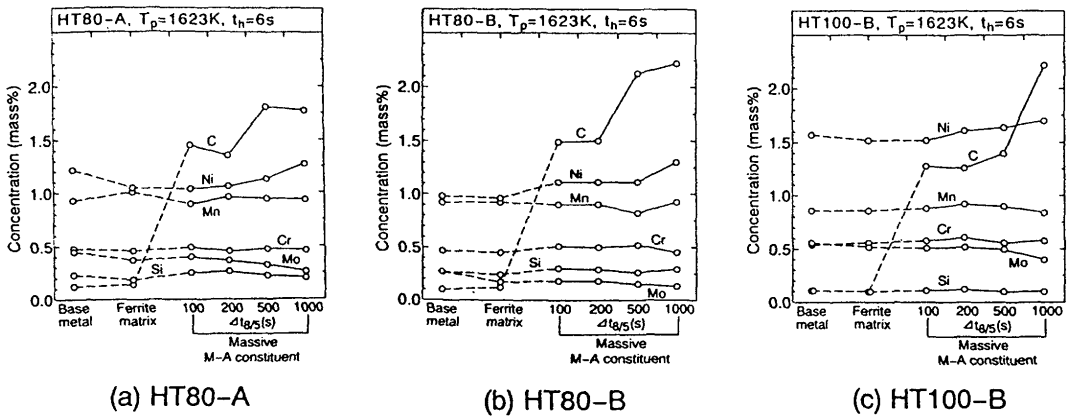

Fig. 48 Change in the composition of massive M-A constituents with $\Delta t_{8/5}$ [58].

microstructure such as microstructure of martensite and distribution of retained austenite[60], in particular with respect to the weld metal and HAZ.

Recently, Matsuda et al.[58, 61, 62], have investigated systematically the fine microstructure of M-A constituent in simulated weld HAZs of 780 MPa and 980 MPa class HSLA steels. They observed two types of cementite in M-A constituent:

(1) coarser, rod-like cementite situated at peripheral regions of the M-A constituent, inside of retained austenite, and retained austenite/martensite boundaries, and

(2) very fine needle-like or dendritic cementite precipitated in the lath martensite.

From its morphology, the coarse rod-like cementite was considered to be precipitated at relatively high temperatures directly from austenite enriched in carbon. The fine needle-like or dendritic cementite was considered to be precipitated during self-tempering of lath martensite in the M-A constituent.

In the massive M-A constituent in weld HAZs of the HSLA steels, plate martensite involving twins, lath martensite of high dislocation density, retained austenite, and cementite were observed. In the elongated M-A constituent, most of the martensite observed was the lath martensite involving dislocation of high density. The plate martensite, retained austenite, and cementite were also observed in the elongated M-A constituent. From many observations, it was concluded that the plate martensite was prevalent in the massive M-A constituent, and the lath in the elongated M-A constituent. It was also concluded that the amount of retained austenite observed in the massive M-A constituent was greater than that observed in the elongated M-A constituent, though the fraction of the retained austenite was much smaller than that of the martensite even in the massive M-A constituent.

From these results, Hrivnak et al.[61] have concluded that the martensite in M-A constituent can have different Ms temperatures and the temperature sequence at which the final product of M-A constituent is formed can be characterized as follows:

-- temperatures at which the structurally-free cementite is precipitated from austenite,
-- the Ms temperature of lath martensite,
-- the Ms temperature of plate martensite, and
-- in between fine cementite can precipitate within the lath martensite during its self-tempering.

5. Formation and decomposition of M-A constituent

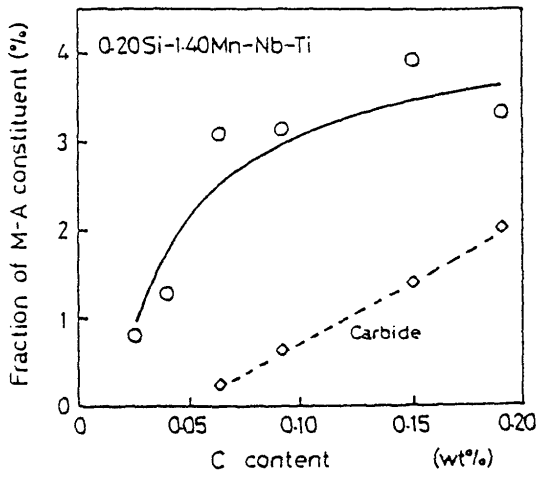

Fig. 50 Effect of C content on fraction of M-A constituent [8].

During ferrite and bainite transformation after welding, C generally redistributes and concentrates in austenite. The M-A constituent that consists of the mixture of martensite and austenite forms by the martensite transformation of the austenite enriched in C at lower temperatures[30, 63], and is detrimental to toughness. Therefore, to improve the toughness of heat affected zone (HAZ) of weld, it is very important to understand the mechanism of formation and decomposition of M-A constituent. The formation and decomposition of M-A constituent are affected by welding thermal cycle as well as by chemical composition. In this chapter, factors that influence the formation and decomposition of M-A constituent are explained.

5.1 Effect of chemical composition on the formation of M-A constituent

5.1.1. Carbon

A lot of research has been reported on the effect of C on the formation of M-A constituent[8, 28, 63]. The C content in M-A constituent is almost independent of the C level of the base metal [8], and estimated to be 0.5-1.5 mass%[8, 37], whereas the amount of M-A constituent greatly changes with C content. **Figure 50** shows the effect of C content on the fraction of M-A constituent. The fraction of M-A constituent increases with C content, especially at low C region[8]. Therefore, the amount of M-A constituent can be reduced by lowering C content of the base metal, which improves the toughness of HAZ [28].

5.1.2. Other elements

1) Mn, Cr, Mo

For the formation of M-A constituent, low Bs temperature is necessary as the C-rich γ phase decomposes into ferrite-cementite aggregate at temperatures about 873 K (600 °C). Therefore, high Mn-Cr-Mo bearing steel easily forms M-A constituent, because these alloying elements decrease Bs temperature[30].

2) Si

In upper and lower bainite transformations, Si retards precipitation of cementite, and C is enriched in the austenite. By reducing the Si content of the alloy, precipitation of cementite is promoted and the width of ferrite laths reduces. This leads to a reduction in the formation of M-A constituent, and improves toughness[64, 65].

3) N

Reduction of N content in the base metal and the weld metal improves toughness, because M-A constituent between the ferrite laths can be changed to pearlite by reducing the N content.

4) Al

Figure 51[26] illustrates the effect of Al on the C profile across ferrite/austenite interfaces in HAZ. By reducing the Al content, the diffusion of C is promoted and carbide precipitates from the high C austenite at lower temperatures. This prevents the formation of M-A constituent in low Al steel.

5) Carbide forming elements

For multipass welding, carbide forming elements Cr, Mo, Nb, and V as well as C tend to form M-A constituent. This is due to the fact that these elements increase the hardenability of the area reaustenized during the second welding thermal cycle, and this promotes the formation of M-A constituent. These elements also retard the decomposition of M-A constituent by preventing C diffusion during the third thermal cycle[4].

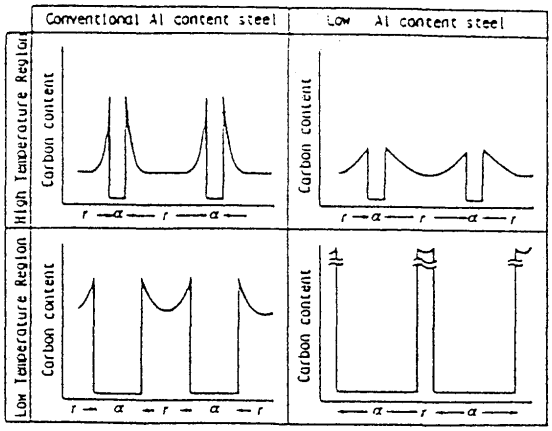

Fig. 51 Schematic illustration of C profile across ferrite/austenite interface in HAZ [26].

6) Ni

The fraction of M-A constituent decreases by reducing Cu and Ni in 500-600 MPa steel[14], because the hardenability becomes lower and less upper bainite forms. On the contrary, by the addition of Ni and Mn in 780 MPa steel, the microstructure changes from upper bainite to lower bainite and martensite, and M-A constituent does not form[11]. In 980 MPa steel with 3.8 mass% Ni, M-A constituent is not observed because of high hardenability[29].

5.2. Effect of welding thermal cycle on the formation of M-A constituent

5.2.1. Maximum reheating temperature

The change in the peak temperature of a single thermal cycle does not affect the formation of M-A constituent[14], although a higher peak temperature leads to a decrease in toughness[4]. Figure 4 illustrates schematically the change of the microstructure according to the peak temperature of the second thermal cycle. When the peak temperature is less than A_{c1} temperature, the microstructure is tempered upper bainite, which is the same as that after first thermal cycle. When the peak temperature is between A_{c1} and A_{c3} temperatures, the M-A constituent forms preferentially along the prior austenite grain boundaries. This M-A constituent is considered to be transformed from the C-enriched austenite region which was reaustenized during the second thermal cycle. At the higher peak temperatures above A_{c3} temperature, the microstructure changes from the mixture of ferrite and pearlite to upper bainite as the peak temperature increases[4, 5].

Figure 52[66] is a schematic illustration showing the formation of M-A constituent when the reheated peak temperature is above A_{c3}. At this temperature, the hardenability of the steel is low and the formation process of M-A constituent is different from that when the steel is heated to the ferrite and austenite region. During heating up to A_{c3} temperature, austenite starts forming from the high carbon region, mainly from the prior austenite grain boundary region (B, C). At temperatures just above A_{c3} temperature, high C regions remain because the temperature is not high enough for C to diffuse uniformly (D), and during cooling, polygonal ferrite and bainitic ferrite transform from low carbon

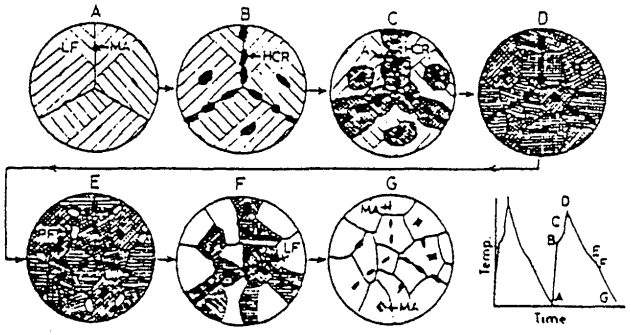

Fig. 52 Schematic illustration of formation of M-A constituent in the low hardenability region [66].

regions (E, F) and finally M-A constituent forms from the remaining high C austenite (G).

5.2.2. Cooling rate

The formation of M-A constituent is greatly influenced by the cooling rate after welding[14, 28-30, 63]. **Figure 53** shows the cooling time range for M-A constituent formation in the simulated HAZ of various strength steels. As the strength level increases, i.e., with the addition of alloying elements such as Ni, Cr, Mo and B, the range shifts to longer times and is broadened. In Figure 16, the number, size and fraction of M-A constituent are shown as a function of cooling time (Tc) from 1073 K (800°C) to 773 K (500°C) for steels of various strength levels. Although the Tc range in which M-A constituent forms is dependent on the strength level of the steel as shown in Fig. 53, there is a clear relationship between Tc and the formation of M-A constituent. As Tc increases, the number of M-A constituent rapidly increases in the smaller Tc region, but is saturated or slightly decreases in the larger Tc region. While the size of M-A constituent is almost constant in the smaller Tc region, it increases with Tc in the larger Tc region. Consequently, the fraction of M-A constituent, which is calculated from the size and number of M-A, steadily increases with Tc[28]. For the single thermal cycle, the fraction and the size of M-A constituent increase with the cooling rate. Figure 18 shows the relationship between cooling time $\Delta t_{8/5}$ and the fraction of M-A constituent. As $\Delta t_{8/5}$ increases, the fraction of M-A constituent increases, and the M-A constituent decomposes partially into ferrite and carbide at very long cooling times $\Delta t_{8/5}$[29].

5.2.3. Heat input

Heat input during welding affects the formation of M-A constituents through the maximum reheating temperature and cooling rate. (See section 5.2.1 and 5.2.2)

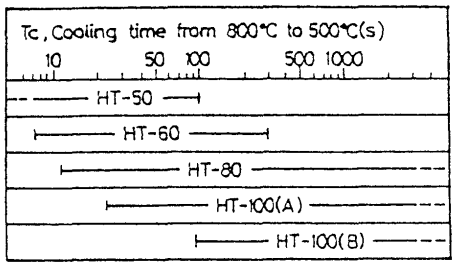

Fig. 53 Cooling time range for the formation of M-A constituent [28].

5.2.4. Multi-thermal cycle

M-A constituent forms during the second thermal cycle (peak temperature 1073 K (800°C) is between A_{c1} and A_{c3}) along the prior austenite grain boundary[5]. **Figure 54** illustrates the formation of M-A constituent during the second thermal cycle whose peak temperature is in the ferrite+austenite region[37]. After the first thermal cycle, carbides precipitate on the coarse prior austenite grain boundary. During the second thermal cycle, austenite forms on the grain boundary (B), and the carbides dissolve into austenite region (C). During cooling from ferrite+austenite region, the austenite region is enriched in C, as the fraction of austenite decreases (D). Finally, the austenite partially transforms into martensite and results in the formation of M-A constituent.

5.3. Decomposition of M-A constituent

5.3.1. Effect of cooling rate

As is mentioned in a previous section, the cooling rate after welding affects the formation of M-A constituent. It also affects the decomposition of M-A constituent formed during cooling. **Figure 55** shows that the fraction of M-A constituent decreases because of its decomposition into ferrite and carbide when the cooling time is more than 50 s[63].

5.3.2. Effect of tempering temperature

M-A constituent decomposes into a fine precipitated phase by the third thermal cycle at 723 K (450°C)[29]. The fraction of M-A constituent decreases when the peak temperature of the third thermal cycle is below A_{c1}, because the M-A constituent decomposes. Nakao et al. observed that M-A constituent partially decomposes by precipitating carbide at 573-673 K (300 - 400 °C), and almost fully decompose at 873-973 K (600 - 700°C)[37]. M-A constituent also decomposes into ferrite and carbide following the post weld heat treatment (PWHT). As the PWHT temperature and time increase, the area of the M-A constituent decreases [39].

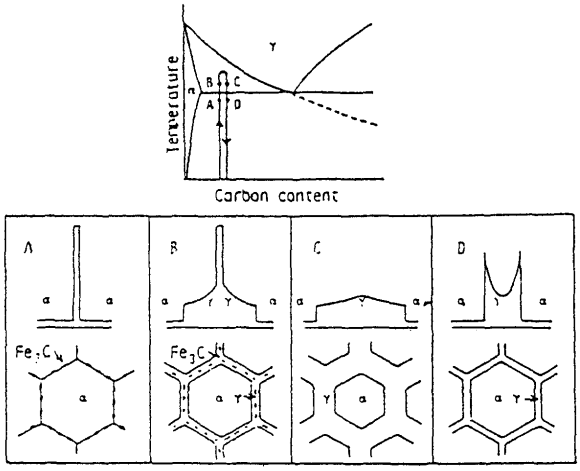

Fig. 54 Schematic illustration ofthe formation of M-A constituent in $\alpha+\gamma$ region[37].

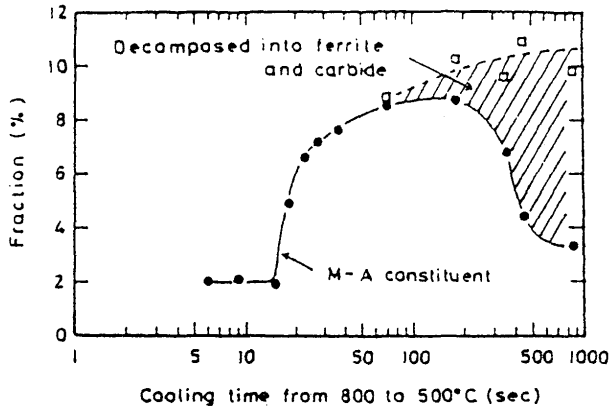

Fig. 55 Effect of cooling rate on the formation and decomposition of M-A constituent [63].

5.3.3. Effect of chemical composition

Carbon and other carbide forming elements retard the decomposition of M-A constituent during the third thermal cycle [4], because these elements prevent the diffusion of C and retard the decomposition of M-A constituent.

6. Conclusion

A review of the M-A constituent in weldments has been made on the basis of papers reported mainly in Japan from 1981 to 1994. Most of the papers are concerned with the toughness impairment of the weld HAZ by the M-A constituent, whereas only few papers are concerned with mechanical properties other than the toughness, mechanical properties of the weld metal, the corrosion resistance properties and so on. A comprehensive understanding of the fine microstructure of the M-A constituent and formation mechanism seem to be still lacking, although many authors have pointed out the importance of controlling the formation of M-A constituent to improve the joint efficiency. The authors suggest the following as future subjects about which more information is needed:

(1) influence of the M-A constituent on the mechanical properties of the weld metal,
(2) influence of the M-A constituent on the corrosion resistance of the weldment,
(3) mechanism of the impairment of the toughness by the M-A constituent -- superimposed effects of mechanical properties of the matrix, and effect of the morphology of the M-A constituent --,
(4) influence of segregation on the formation of the M-A constituent and toughness impairment, and
(5) comprehensive understanding of the fine microstructure of the M-A constituent.

References

1) M.Suzuki, S.Sakui, T.Kojima and I.Watanabe:'High Heat Input Welding of 60kgf/mm2 Grade High Tensile Strength Steel', Quarterly J. JWS, 1-2(1983)p.209 (in Japanese).
2) M.Nakanishi, Y.Komizo and Y.Fukada:'Study on the Critical CTOD Values in the Heat Affected Zone of C-Mn Microalloyed Steel', Quarterly J. JWS, 4-2(1986)p.447 (in Japanese).
3) Y.Horii: 'Recent Development on Controlling the Microstructure and Toughness of Low Alloy Weldments', 128th Nishiyama Memorial Lecture, ISIJ, (1989)p.56.
4) T.Haze, S.Aihara, Y.Ohno, K.Uchino, Y.Kawashima, Y.Tomita, R.Chijiiwa and H.Mimura: 'Steel Plate with Superior Toughness for Offshore Structure', SEITETSU KENKYUU, 326(1987)p.36 (in Japanese).
5) T.Haze, S.Aihara, Y.Hagiwara, Y.Kawashima, K.Uchino, S.Tomita and R.Chijiiwa: 'Influence of the Local Brittle Zone on Critical CTOD of Weld HAZ in 50 kgf/mm^2 Tensile Strength Steels', Tetsu-to-Hagane, 74-6(1988)p.1105 (in Japanese).
6) T.Haze, S.Aihara, Y.Hagiwara, K.Uchino, Y.Kawashima, S.Tomita and R.Chijiiwa:'A Study on Factors Controlling Critical COD Value of Welded Joints of High-Tensile Strength Steel', J.SNAJ, 162(1987)p.447.
7) S.Machida, T.Miyata, M.Toyosada and Y.Hagiwara:'Study on CTOD Test Method of Weldments', ASTM Symp. Fatigue and Fracture Testing of Weldments, ASTM(1988).
8) Y.Komizo and Y.Fukada:'CTOD Properties and M-A Constituent in the HAZ of C-Mn Microalloyed Steel', Quarterly J. JWS, 6-1(1988)p.41 (in Japanese).
9) Y.Komizo and Y.Fukada:'Fracture Toughness and M-A Constituent in the Heat Affected Zone of C-Mn Microalloyed Steel', Suiyokwai-Shi, 20-9(1987)p.621 (in Japanese).
10) K.Uchino and Y.Ohno:'Effect of Cooling Rate on Formation of M-A Constituent', Tetsu-to-Hagane, 72-12(1986)s1159 (in Japanese).

11) S.Endo, M.Suga, H.Tsukamoto, K.Matsumoto and H.Ishikawa:'Effect of Microstructure on HAZ Toughness of Steel Plate for Offshore Structure', Tetsu-to-Hagane, 72-12(1986)s1157 (in Japanese).
12) N.Akiyama, K.Iwai, S.Takashima, K.Abe, H.Kaji and M.Kanou:'Effect of Mn/C on Base Metal Property and Weldability of TMCP HT50 Steel Plate', Symp. Welding Metallurgy of TMCP Steel, JWS, (1985)p.93.
13) R.Someya, S.Suzuki and M.Nishizawa:'Effect of microstructure on HAZ Toughness', Tetsu-to-Hagane, 72-13(1986)s1538 (in Japanese).
14) T.Tagawa, T.Miyata, S.Aihara and K.Okamoto:'Influence of Martensitic Islands on Fracture Toughness and Strength of Weld Heat-affected Zone', Tetsu-to-Hagane, 79-10(1993)p.1176 (in Japanese).
15) F.Kawabata, N.Itakura, H.Jing, K.Amano, F.Minami and M.Toyoda:'Morphological Effect of Local Hard Zones on Fracture Toughness of Weld HAZ', J.SNAJ, 173(1993)p.349.
16) S.Aihara and K.Okamoto: 'Influence of Local Brittle Zone on HAZ Toughness of TMCP Steels', Int.Conf. The Metallurgy, Welding, and Qualification of Microalloyed (HSLA) Steel Weldments, AWS, (1990)p.402.
17) T.Tsuzuki, S.Tomita†and R.Yamaba:'Effect of Grain Size and Structure on A_{c1} Embrittlement of HAZ', Tetsu-to-Hagane, 72-13(1986)s1537 (in Japanese).
18) T.Fujita, A.Yoshie and H.Morikawa:'Formation of M-A Constituent in the Plate Produced with Thermo-Mechanical Control Process and its Effect on Toughness', CAMP-ISIJ, 1-6(1988)-1737.
19) T.Tagawa, T.Miyata, S.Aihara and K.Okamoto:'Analysis of Embrittlement in Weld Heat-affected Zone due to Formation of Martensitic Islands by Local Criterion Approach', Tetsu-to-Hagane, 79-10(1993)p.1183 (in Japanese).
20) M.Nakanishi, Y.Komizo and Y.Fukada:'Effect of Segregation on Critical CTOD Value in HAZ of HT50 Steel', National Meeting JWS, 38(1986)p.88 (in Japanese).
21) Y.Kawashima, and K.Imano:'Effect of Alloying Elements on Toughness of Simulated HAZ', Tetsu-to-Hagane, 72-5(1986)s620 (in Japanese).
22) Abe:Committee of Welding Metallurgy, WM-1144-86(1986).
23) M.Nakanishi, Y.Komizo and Y.Fukada:'Effect of Chemical Compositions on CTOD Property in HAZ', National Meeting JWS, 37(1985)p.216 (in Japanese).
24) S.Aihara, T.Hasegawa and K.Okamoto:'Influence of Si on Formation and Decomposition of Martensitic Island in Multi-pass Weld HAZ', CAMP-ISIJ, 4(1991)-1886.
25) F.Kawabata, K.Amano, M.Toyoda and F.Minami:'Effect of Interpass Temperature on Decomposition of Martensite-Austenite Constituent in Local Brittle Zone', CAMP-ISIJ, 4-3(1991)-790.
26) Y.Fukada and Y.Komizo:'Effect of Al Content on Critical CTOD Properties in Heat Affected Zone of C-Mn Microalloyed Steel', Quarterly J. JWS, 10-3(1992)p.409 (in Japanese).
27) K.Arimochi and K.Isaka:'Development of LBZ Free Technologies', Symp. Welded Structure'91, JWS, (1991)p.54.
28) Y.Kasamatsu, S.Takashima and T.Hosoya : 'Influence of Martensite-Austenite Constituent on Toughness of Heat Affected Zone of High-Strength Weldable Structural Steels', Tetsu to Hagane, 65-8(1979), p.1222-1231 (in Japanese).
29) H.Okada, F.Matsuda and Z.Li : 'The behavior of M-A Constituent in Simulated HAZ with Single and Multiple Thermal Cycle', Quarterly Journal of JWS, 12-1(1994), p.126-131 (in Japanese).
30) Y.Hirai : 'Effect of Martensite-Austenite Constituent on Toughness of High Strength Steel Weldments', Journal of JWS, 50-1(1981), p.37-46 (in Japanese).
31) F.Kawabata, K.Amano, N.Itakura, F.Minami, M.Toyoda and H.Jing : 'Morphologic Effect of Local Hard Phase on Toughness of Local Brittle Zone', Proc. of the Workshop on Strength Mismatching and Its Control, Tokyo, July, 1992, (IIW Doc. X-1254-92), p.1-11.
32) F.Minami, H.Jing, M.Toyoda, F.Kawabata and K.Amano : 'Effect of Local Hard Zone on Fracture Initiation of Weld HAZ', Proc. of the Workshop on Strength Mismatching and Its Control, Tokyo, July, 1992, (IIW Doc. X-1254-92), p.23-34.
33) F.Kawabata, K.Amano, N.Itakura, F.Minami, M.Toyoda and H.Jing : 'Morphological Effect of Local Hard Zones on Fracture Toughness of Weld HAZ', Proc. of the 2nd Workshop on Constraint Effects on the Structural Performance of Welded Joints, Osaka, September, 1994, (IIW Doc. X-1300-94), p.126-132.
34) F.Matsuda, K.Ikeuchi and J.Liao : 'Weld HAZ Toughness and Its Improvement of Low Alloy Steel SQV-2A for Pressure Vessels (Report 1)', Trans. JWRI, 22-2(1993), p.271-279.
35) T.Shiwaku, Y.Kobayashi, M.Shimizu, M.Toyoda and F.Minami : 'Metallurgical Factors on Toughness in Intercritically Reheated HAZ of Low-C Low-Alloy Steel', Proc. of 4th Int. Conf. on ISOPE, Osaka, vol.IV, (1994), p.215-221.
36) T.Kubo, O.Furukimi, T.Yamaura and Y.Saitoh : 'Effect of C, Nb and Ni on the Toughness of Heat Affected Zone of Welded Joints in Steels of Storage Tanks for Low Temperature Use', Quarterly Journal of JWS, 8-2(1990), p.228-235 (in Japanese).
37) Y.Nakao, H.Oshige, S.Noi and Y.Nishi : 'Distribution of Toughness in HAZ of Multi-Pass Welded High Strength Steel', Quarterly Journal of JWS, 3-4(1985), p.773-781 (in Japanese).
38) F.Matsuda, K.Ikeuchi, J.Liao and H.Tanabe : 'Weld HAZ Toughness and Its Improvement of Low Alloy steel SQV-2A for Pressure Vessels (Report 2)', Trans. JWRI, 23-1(1994), p.49-57.
39) H.Okada, F.Matsuda, K.Ikeuchi and Z.Li : 'Decomposition Behavior of M-A Constituent and Recovery of Toughness', Quarterly Journal of JWS, 12-3(1994), p.398-403 (in Japanese).
40) H.Okada, F.Matsuda, K.Ikeuchi and Z.Li : 'Toughness Recovery for Weld HAZ by Post Weld Heat Treatment', Quarterly Journal of JWS, 12-4(1994), p.521-527 (in Japanese).
41) H.Okada, F.Matsuda, K.Ikeuchi and I.Hrivnak : 'Effect of M-A constituent on fracture behavior of weld HAZ with high heat input in 780 and 980MPa class HSLA steels', Proc. of 2nd Workshop on Constraint Effects on the Structural Performance of Welded Joints, Osaka, September, 1994, (IIW Doc. X-1300-94), p.134-141.
42) M.Nakanishi, N.Komizo and M.Tanaka: 'Improvement of toughness of High Strength Steel Weld Metal', J. of the JWS, 52-2(1983)p.57-63 (in Japanese).
43) Y.Ito, M.Nakanishi and N.Komizo: 'Crack Opening Displacement Properties on Submerged Arc Weld Metals', J. of the JWS, 47-9(1978)p.650-656 (in Japanese).

44) T.Koshio, M.Ootawa and T.Tanigaki et al.: 'Development of the high titanium bearing covered electrode',IIW Doc.II-955-81.
45) Y.Kikuta,T.Araki and M.Yoneda: 'The Controlling Factors of Reheated Zone Toughness for Si-Mn and High Strength Low Alloy Weld Metal on Multipass Welding', The 4th Int. Sympo. of the JWS, Nov. 1982, Osaka.
46) Y.Kikuta, T.Araki and A.Okubo et al.: 'Effect of Microstructure on Toughness of Reheated Multi-pass Weld Metal of High Carbon Steels', Preprints of national meeting of the JWS,29(1981)p.1905-1906 (in Japanese).
47) Y.Horii, S.Ohkita and M.Wakabayashi et al.: 'Improvement of Weld Metal Toughness at Reheated Region', Int. conf. of PACOMS,1989,Soule.
48) Y.Horii, S.Ohkita and M.Wakabayashi et al.: 'Study on the Toughness of Large-Heat Input Weld Metal for Low Temperature Service TMCP Steel', Nippon Steel Technical Report No.37-4(1988)p.1-9.
49) Y. Miyata ,M .Kimura,Y. Saito and C. Shiga: 'Effect of microstructure on local corrosion of HSLA steel welds', CAMP, 4-3(1991)p.808.
50) Y. Miyata ,M .Kimura,Y. Saito and C. Shiga: 'Local corrosion in heat affected zone of YP440 MPa HSLA steel', CAMP,5-6(1992)p.1983.
51) Y.Kikuta,T.Araki and M.Yoneda: 'Influence of island martensite on delayed fracture.1', Preprints of the national meeting of J.W.S. 37(1985)p.194-195 (in Japanese).
52) Y.Kikuta,T.Araki and M.Yoneda: 'Influence of island martensite on delayed fracture.2', Preprints of the national meeting of J.W.S. 39(1986)p.176-177 (in Japanese).
53) Y.Yamane and F.Kawabata, O.Furukimi: 'Effect of amount of M-A constituent on sulfide stress cracking of steel for line pipe', CAMP,7-3(1994)p.729.
54) H.Okada, K.Ikeuchi, F.Matsuda, and I.Hrivnak : Quarterly J. Japan Weld. Soc., 13-1(1995) 99-105 (In Japanese).
55) V.Biss and R.L.Cryderman : Metall. Trans., 2-8(1971), 2267-2276.
56) B.Josefsson and H.O.Andren : Int. Conf. on Recent Trends in Welding Science and Technology, Gatlinburg, Tennessee, (1989), p.243.
57) F.Kawabata, K. Amano, N.Itakura, F.Minami, M.Toyoda and H.Jing : Proc. The Workshop on Strength Mismatching and Its Control, (1992) 23-34.
58) H.Okada, K.Ikeuchi, F.Matsuda, I.Hrivnak and Z.Li : Quarterly J. Japan Weld. Soc., 12-2(1994) 236-242 (In Japanese).
59) L.J. Habraken and M. Economopoulos: Proc. Symp. Transformation and Hardenability in Steels, Climax Molybdenum Company, Michigan, (1967), 69.
60) T. Bold and B. Garbarz: Prac. Metall., 17(1980), 338.
61) I. Hrivnak, F. Matsuda, and K. Ikeuchi: Trans. JWRI, 21(1992), 149.
62) I. Hrivnak, F. Matsuda, Z. Li, K. Ikeuchi, and H. Okada: Trans. JWRI, 21(1992), 241.
63) H. Ikawa, H. Oshige and T. Tanoue: 'Study on the Martensite-Austenite Constituent in Weld-Heat Affected Zone of High Strength Steel', Journal of JWS, 49-7 (1980), p.467-472 (in Japanese).
64) Y. Ohtani, S. Watanabe, Y. Kawaguchi and Y. Yamaguchi: 'Improvement in Toughness of Large Heat-Input Weld Bond of 60 kgf/mm^2 Grade High Tensile Strength Steel Plates due to Boron Addition and Low Silicon Content', Tetsu-to Hagane, 64-14 (1978), p.2205-2214 (in Japanese).
65) O. Tanigawa, H. Ishii, N. Itakura, K. Amano, Y. Nakano and F. Kawabata: 'The 420 MPa and 500 MPa Yield Strength Grade Steel Plates with Excellent HAZ Toughness Produced by TMCP for Offshore Structure', Kawasaki Steel Giho, 25-1 (1993), p.13-19 (in Japanese).
66) Y. Nakao, H. Oshige, S. Noi and Y. Nishi: 'Mechanism of Formation of Microstructure in Low-Hardenability zone in Weld-Heat Affected Zone', Quarterly Journal of JWS, 5-3 (1987), p.415-422 (in Japanese).